Liquid drop dynamics under the effect of an induced Horizontal Wettability Gradient

A Thesis submitted in partial fulfillment of the requirements for the Degree of

Bachelor of Technology

in

Mechanical Engineering

by

Suseet Panigrahi (Roll No. 109ME0401)

under the guidance of

Dr. Suman Ghosh

Department of Mechanical Engineering
National Institute Of Technology
Rourkela – 769008

National Institute of Technology

Rourkela

CERTIFICATE

It is certified that the thesis entitled "**Liquid drop dynamics under the effect of an induced Horizontal Wettability Gradient**" submitted by **Suseet Panigrahi** (Roll No.109ME0401) in partial fulfilment of the requirements for the award of **Bachelor of Technology Degree** in **Mechanical Engineering** at National Institute of Technology, Rourkela, is an authentic work which has been strictly carried out under my supervision and this work has not been plagiarised from elsewhere to the best of my knowledge.

Place: Rourkela

Date:

Dr. Suman Ghosh
Assistant Professor
Department of Mechanical Engineering
National Institute of Technology, Rourkela

ACKNOWLEDGEMENT

I am highly indebted to my guide Dr. Suman Ghosh for giving me an opportunity to work under his guidance. Like a true mentor, right from the beginning, throughout the entire duration, and through every step of my work, he motivated and inspired me to move further. A person with firm determination and hope, he is the one without whom this work could not have seen its day.

I am also grateful to Mr. Sukant, Mr. Ajoy and Mr. Gaurav, for assisting me in my task and helping me rectifying the mistakes in my methodology. I also extend my thanks to the supportive staff of Mechanical Department for providing me necessary facilities to accomplish this project.

Last but not the least, I would like to express my profound gratitude to the almighty and my parents for their blessings and support without which this task could have never been accomplished.

Suseet Panigrahi

109ME0401

CONTENTS

Index of Figures

List of symbols

Symbols	Description
P	Density(kg/m^3,lb/ft^3)
Y	Overall velocity vector (m/s, ft/s)
E	Total energy, activation energy (J, kJ, cal, Btu)
P	Pressure (Pa, atm, mm Hg, lbf /ft2)
G	Gravitational acceleration (m/s^2, ft/s^2); standard values = 9.80665
F	Force vector (N, lbf).
k_{eff}	Effective Thermal conductivity (W/m-K, Btu/ft-h-F).
T	Temperature (K, $^\circ$C, $^\circ$R, $^\circ$F).
S_h	Volumetric heat source(j/m^3).
T	Time(s).
α_q	Volume fraction of qth phase.
ρ_q	Density of qth phase (kg/m^3, lbm/ft^3).
E_q	Energy of qth phase.
μ	Dynamic viscosity (cP, Pa-s, lbm/ft-s).
K	Turbulence kinetic energy.
ε	Dissipation rate.
c_1,c_2,c_μ	Constants.
σ_k	Turbulent Prandtl numbers for k.
σ_ε	Turbulent Prandtl numbers for ε.

ABSTRACT

A liquid drop when placed over a rigid surface tends to obtain an equilibrium shape with minimum surface energy. This phenomenon is a consequence of a number of parameters like density, contact angle, surface tension and volume of the droplet. The drop under consideration would remain static under the absence of any external force and contact angle gradient (or wettability gradient). With the effect of the above factors, it may so happen that the drop may self-propel itself towards a direction which would minimize its surface energy. Depending upon the strength of the above factors, it may be even possible to move up the drop in any desired direction as per applications requirements like cooling of hot spots in electronic equipments like laptops, controllers, etc. involving micro fluids. The present study is based upon the effect of wettability gradient over a liquid drop with reference to its movement using VOF model with Finite Volume Method. Finally horizontal drop mobility curves representing wettability gradient versus volume have been plotted. Further attempts have been made to study some other characteristics of this phenomenon.

Keywords: Computational Fluid Dynamics, Volume of Fluid, Wettability Gradient, Multiphase, horizontal Mobility Curve.

Chapter 1

1. INTRODUCTION AND LITERATURE REVIEW:

In this section the problem has been first introduced and then an exhaustive literature survey has been made. After that the gaps in the literatures have been point out and at last, aims and objectives for the present work have been clearly defined.

1.1 Introduction:

The profound applications based on controlled and regulated movements of liquid drops over artificially created surfaces have been finding tremendous growth, starting from their most extensive use in cooling of hotspots in electronic circuits, micro pumps, printing and coating techniques (especially over unreachable places), hydrophobic surface designs, valve regulating mechanisms and has a future prospect to be used in controlled nuclear and other micro reactions in order to have an efficient control over the rate of reaction. Even natural biological processes like photosynthesis, absorption of minerals, blood circulation and various other essential phenomena inherently depend on the process. The well controlled regulated movement of the liquid phases, their intermixing, and regeneration, when fully controlled could enhance the capability of the phenomena to have highly efficient (owing to their low energy requirements) and sophisticated applications.

1.2 Liquid Drop Dynamics: When a drop of liquid is placed over a surface, the final shape it obtains does depend upon a number of factors that are functions of the nature of the fluid, the surface and the surrounding atmosphere. In other words the governing factors include surface tension, material properties, homogeneity of the materials, nature of interaction between them, gravity effects, surrounding medium and geometry of the surface, neglecting external forces. The dynamics of a small liquid drop is a bit different than that of the bulk fluid because of the surface tension force dominating over the inertial and viscous forces. The movement of a drop can be influenced by factors like gravitational force, thermal gradient or wettability gradient which may be induced artificially.

1.3 Wettability Gradient: The contact angle at a given point of contact along the contact line between a solid and a liquid surrounded by a fluid medium is the angle between the tangent planes to the liquid and the solid surfaces at that point and is measured within the liquid side, by convention as depicted in Figure 1. The variation of contact angle over the diametrical length along the contact surfaces denote wettability gradient with unit °/mm. If a contact angle gradient (wettability gradient) is established over a liquid drop surface, there occurs an imbalance of surface tension over the circumferential plane of a droplet base, resulting in a net unbalanced force in the direction of increasing contact angle, hence, the center of mass of the system tries to attain the minimum equilibrium position and a net rearrangement of the particles occur and if this driving force overcomes the inertial and viscous forces, it finally results in the movement of the drop. Due to the extreme values of surface to volume ratio, conventional methods cannot be adopted for the movement of droplets. The nature of the motion is determined by the balance between the influencing force and the resisting hydrodynamic force from the solid surface and the surrounding gaseous medium. Similarly, if there is a variation of contact angle of a liquid drop with fixed volume, over the circumferential plane, the drop assumes an asymmetrical shape along it with a net unbalanced force. Contact angle hysteresis refers to the difference in contact angles at the advancing (Θ_a) and receding (Θ_b) faces of the drop. If the critical contact angle difference ($\Theta = \Theta_a - \Theta_b$) exceeds beyond a certain value, governed by a number of factors like density, properties of surrounding, surface tension, gravity, contamination, etc. , there exists an imbalance of surface forces and the drop tries to self-propel itself to minimize its surface energy.

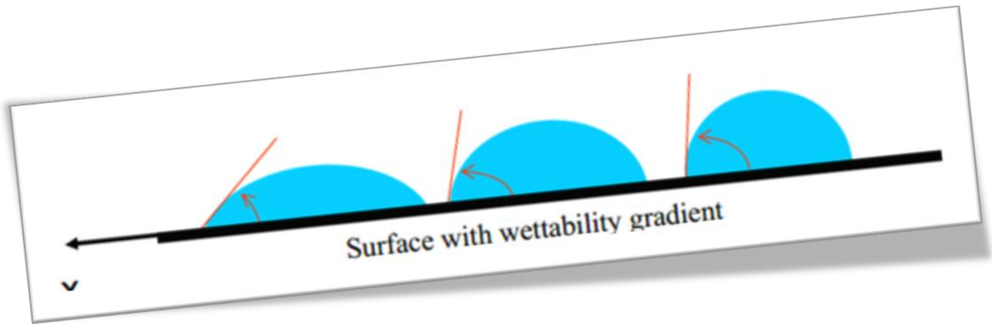

Figure 1: Description of Contact Angles and Wettability Gradient.

1.4.1 Literature Review:

The first official theory established dates back to 1978 when Greenspan (1978) [16] inspired by the work of Carter, developed a model describing the forces acting on a small viscous droplet based on lubrication equations and over a dynamic contact angle. The cases of spreading of a circular droplet, creeping of a droplet on a coated surface towards a region of greater adhesion and distortion of droplet shape owing to surface contamination have been analyzed. Two specific problems: shape of the largest bubble drop over an inclined surface and shape and speed of the drop when these conditions exceed has been demonstrated by Dussan et al. (1983) [10]. A method had been proposed by Gingold et al. (1977) [14] to use of statistical technique to obtained analytical expression for a physical variable from a known distribution of fluid element. This method has been used to produce the structure of uniformly rotating and magnetic polytropes. The effect of thermal and chemical gradients on the motion of droplets on solid surfaces has been explained quantitatively by Brochard (1988) [3] in terms of spreading coefficient for partial wetting and complete wetting fluids. The impact of Marangoni effect on the motion has been depicted. The unbalanced “young force” was being used to estimate the driving force. The uphill motion of water droplet by creating hydrophobic and hydrophilic gradients over a small distance apart on the surface of a polished silicon wafer by exposing it to the diffusing front of a vapour of decylthrichlorosilane has been experimentally demonstrated by Chaudhury and Whitesides (1992) [4]. In order to move the droplet, the hysteresis in contact angle on the surface has to be low. The induced migration of a small drop on a solid surface by thermocapillary forces, establishing a surface tension gradient has been theoretically demonstrated by Ford and Nadim (1993) [11]. Using lubrication theory the study describes the behavior of a droplet modeled as infinitely long strip of finite width and arbitrary height profile. But the analysis only provides the steady state value of the migration velocity of the drop and under given final height profile. Fluid mechanics has been applied by Shikhmurzaev (1997) [25] to predict the dynamic spreading of a macroscopic liquid droplet where the energies associated with the volume are dominant and on reducing the droplet size to sub-millimeter level, surface energy becomes a dominant factor. Morris and Fox (1997) [22] have implemented a three dimensional smooth particle hydrodynamics (SPH) simulator to model grain scale fluid flow (low Reynolds Number) in porous media to demonstrate the accuracy of the results and the versatility of the approach. The use of non-Newtonian flow properties to slow down the retraction sufficiently to completely inhibit rebound has been demonstrated by Bartolo et al. (1997) [1]. It was explained that the slowing down is due to non-Newtonian normal stresses generated near the moving contact line of the droplet. It has been discovered by Gau et al. (1999) [15] that chemically structured faces lead to morphological wetting transitions at which the wetting layer changes its shape in a characteristic and abrupt manner. He plotted the morphology diagram as a function of the aspect ratio of the channel and the contact angle. A microfluidic capillary system that autonomously transports aliquots of different liquids in sequence has been demonstrated by Gallardo et al. (1999) [12] observed a rapid motion of similar water drops when condensation occurred on cold surfaces has been observed by Daniel et al. (2001) [6]. It has been demonstrated by Beltrame et al. (2001) [2] that the onset of droplet motion on non-ideal real substrates under lateral driving is strongly influenced by substrate defects and a finite driving force is necessary to overcome the pinning influence of micro scale heterogeneities. The movement of a liquid drop towards the more wettable part of the gradient with typical speeds of 1-2mm/s has been experimentally demonstrated by Daniel and Chaudhury (2002) [7]. It has been claimed that the observed lower speed was due to the effect of contact angle hysteresis over the driving force. Application of periodic force to a drop resting on such a gradient surface enhances the force along the gradient. The driving force due to a contact angle gradient over a drop using a flexible glass micro needle was directly measured by Hitoshi and Satoshi (2003). It has been concluded that a balanced drag force with the driving force need to be reconstructed, using a new concept of solid like friction. The effects of size of the chains composed of the drop and initial velocity of the drop on the drop terraced spreading have been studied by Wu et al. (2003) [27]. The chain size effects on the base radius of drop have been studied at zero initial velocity. The longer the chain, the slower is the spreading. With a nonzero initial velocity, the drop base radius increases with increasing initial velocity before the drop splits into smaller separated drops. Experiments have been performed over a variety of liquids by Daniel et al. (2004) [6] and the results reported the enhanced velocities by vibrating the substrates. The movement of a drop as a result of the hydrodynamic force experienced by a spherical cap drop over a solid surface with a wettability gradient has been demonstrated by Subramanian et al. (2005) [26]. Experiments have been reported by Grand et al. (2005) on the shape and motion of millimeter sized droplets sliding down a plane in a situation of partial wetting. One of the solutions has been based on an approximation of shape as a collection of wedges and the other based on the lubrication theory which is good when the length scale of the drop is large as compared with the slip length. A comparative study of contact angle measurements over a variety of polymeric materials and its hysteresis behavior of static and dynamic contact angles was made by Krasovitsky (2005). An asymptotic model using lubrication theory has been proposed by Pismen and Thiele (2006) [24] to demonstrate the motion of a drop over a gradient surface. Experimental results on the motion of tetraethylene glycol drops in a wettability gradient present on a silicon surface with a developed theoretical model have been verified by Subramanian et al. (2006) [26]. Experiments have been performed on the motion of drops of tetraethylene glycol in a wettability gradient present on a silicon surface and these are compared with recently developed theoretical model by Moumen et al. (2006) [23] according to which, the velocity of the drops are a strong function of position along the gradient. To explain this behavior a quasi-steady theoretical model has been given which balances the local hydrodynamic resistance with the local driving force .It was shown that a model in which the driving force is reduced to accommodate the hysteresis effect inferred from the data is able to remove most of the discrepancies between observed and predicted velocities. Contact angle hysteresis on chemically patterned and super hydrophobic surfaces, as the drop volume is quasi statically increased and decreased both two (cylindrical drops) and three (spherical drops) dimensions have been investigated by Kusumaatmaja et al. (2007) [21] using analytical and numerical approaches to minimize the free energy of the drop. Axisymmetric droplet spreading has been investigated by Ding et al. (2007) [9] numerically at relatively large rates of spreading, such that inertial effects also have a role. Results have been presented for the apparent contact angle as a function of dimensionless spreading with various parameters like Ohnesorge number, slip length and initial conditions. The results indicate that there is no such universal relation when inertial effects are important. In two dimensions, the result obtained reveals that a slip, jump, stick motion of the contact line. In three dimensions, this behavior is present, but the position and magnitude of the contact line jumps are sensitive to the details of the surface patterning. For the first time used a numerical technique based on lattice Boltzmann method to investigate the motion of a liquid drop over a chip under a wettability gradient was proposed by Huang et al. (2008) [19]. Theoretically and experimentally the effects of gravity on the shape and focal length changes of liquid droplets with the effect of droplet size and outside atmospheric conditions have been demonstrated by Hongwen et al. (2010) [18].The motion of a liquid drop over a surface using a 3D technique that combines diffuse interface in a smoothed particle hydrodynamics simulation to study the internal fluid structure and the contact line dynamics has been demonstrated by Das and Das (2010) [5]. The study reveals the impact and interdependence of a variety of factors like volume, inclination and strength of the wettability gradient over the movement of the droplet.

1.4.2 Gaps in the Literature:

As could be inferred from above, a very few theoretical models have employed the lubrication theory and a few of them are perfectly able to correlate the experimental results with those of the modeled ones. The main experiments of Daniel et al. (2001, 2002, 2004) does not compares the predictions from any theory they measured. Inspite of the advancements in the field of dynamics of a drop, as can be seen, not much advancement has been made to study the feasibility and accuracy of the computational fluid dynamics model to investigate and correlate the theoretical results with the observed motions. Unfortunately not many efforts have been made to study the dynamics of a drop under the effect of an external induced wettability gradient. Besides, very few theories above have been accurately able to describe the observed velocities under different boundary conditions and the changes in their behavior as a consequence of alteration in external forces. Hence there is a need for a systematic study and analysis on the overall dynamics of bubble drop movement under the variance of external effects and their correlation with the observed behavior for an efficient knowledge over the above phenomena.

1.5 Aims and Objective:

The present work undertaken has been based on the application of Computational Fluid Dynamics method on the Volume of Fluid model which has been used to analyze the dynamics of the motion of drop movement over a horizontal surface to establish the relationship between the obtained inference and their convergence with the observed ones. The objective is to generate a sort of empirical relationship between the governing criteria (wettability gradient) and its consequence on the dynamics of the drop, which could serve as a reference guide in applications requiring their use. In the first section of the work, the motive was to observe the intermediate stages passed through by a drop (water) before attainment of equilibrium shape, with a fixed contact angle defined over its surface as the boundary conditions.

1.6: Organization of Thesis:

The entire thesis is divided into seven chapters:

First chapter is all about the introduction about the present work, pre-ideas and knowledge about the terms associated. It includes a thorough literature survey undertaken before anf during the continuation of the project, their shortcomings and gaps associated with them which gives an insight about the present scope. It also includes objective and a brief description about the overall work.

Second Chapter relates to the definition of problem statement on which the present work has been based on

Third Chapter denotes the methodology adopted, governing equations, boundary conditions, type of solver uses and method of solution approach along with a detailed step-by-step procedure description

Fourth Chapter is the complete description of the results obtained in tabular, pictorial and graphical forms

Fifth Chapter is a complete analysis of the results obtained above along-with proper description about anomalies that have incurred. Also the result of a static drop with an initially assumed hemi-spherical shape while attaining its equilibrium shape has been plotted with respect to time intervals.

Sixth Chapter relates the scope of future work that could be undertaken based upon the results obtained and the subject itself

Seventh Chapter tabulates a complete set of references considered

Chapter 2

2. PROBLEM STATEMENT:

Computational Fluid Dynamics using the Volume of Fluid model has been used to numerically analyze the movement of a water drop over a solid surface (steel) under the effect of a predefined linearly distributed wettability gradient. The drop would self-propel itself in order to minimize its surface energy and if the variance in contact angle, i.e. wettability gradient is strong enough, the drop may be forced to propel up over an inclined or an uneven surface or restrict the movement of a sliding drop as per the requirement. Similarly, drops of varying volumes has been taken as reference and by using a manually defined UDF (user-defined function) the movement of the droplet has been analyzed to find out the critical gradient value at which a drop of specific volume just starts to propel over a horizontal plane and the results have been plotted to determine the effect of this parameter on the movement of the drop. Considering an application, e.g., the effect of strength of implied wettability gradient on the velocity of a drop, the present results could serve as a reference to control the rate of movement. As the systems being considered here are of microscopic dimensions, accuracy of the results has an effect on the efficiency in their applications. In the first part of analysis, the focus is to analyze the shapes the droplet acquires at specific time intervals while attaining equilibrium shape from an initially assumed hemi-spherical shape as the initial value of the solution.

Chapter 3

3. METHODOLOGY:

The present project has been based on results obtained by application of analysis softwares, viz. gambit for modeling and fluent (version 6.3) for processing and simulation. In all of the cases, the models of the profile surface have been generated, implicating different boundary conditions. Geometric models of cuboid representing the system (drop) and the surrounding medium (atmospheric air) have been modeled and meshed with a size sufficiently small such that the accuracy of the results obtained would be within the desired limit(assuming a thumb rule that the drop should contain at least eight grids diametrically). The size of the system considered is such that accuracy of result is not affected by it. The bounding surfaces of the system have been defined by names, and the top surface has been defined as open to atmosphere. The mesh files were imported to Fluent in 3d version and material properties, phases, surface tension values were defined. An unsteady pressure-based solver, using laminar flow model has been adopted with gravity defined as acting downwards. In the first phase of analysis, the contact angle over the contact length around the periphery has been defined with a constant value at the boundary conditions panel. In the second phase, a UDF source code was invoked and interpreted using the default interpreter and was hooked to boundary conditions (bottom surface of the cuboid model in contact with the drop). The zones representing the two phases were marked, and assigned the material properties by patching. A surface plane was defined to mark the movement of the drop over time. Using the PISO solver, the solution was initialized. The Case and Data files were set to be saved at appropriate time intervals to observe the movement. The time step size, residual criteria and the no of iterations per time step has been set and the initial solution was iterated till a finite time duration was obtained. The nature of the movement of the drop has been studied. The process has been repeated a number of times with incremental increase in the strength of the wettability gradient for a specific volume of the liquid drop, till the drop just starts to move.

3.1 Numerical calculation:

The computational approach adopted in the present study is based on finite volume method of the three dimensional unsteady pressure based Navier-Stokes equation with Volume of Fluid model and laminar flow model. VOF model is used when there are two or more immiscible fluids are present to track and locate the fluid- fluid interface. Here all the fluid shared the same single set of equations, and the volume fraction of each of the fluids in each computational cell is tracked throughout the domain. A single momentum equation has been used for both the fluid i.e. water and air.

3.1.1 Governing Equation:

The different governing equations applied are:

(1) The Momentum Equation:-In VOF model a single momentum equation has been used throughout the domain and it is given by,

$$\frac{\partial}{\partial t}(\rho v) + \nabla.(\rho.v.v) = -\nabla p + \nabla.[\mu(\nabla v + \nabla v)] + \rho g + F \quad \ldots(1)$$

It depends on volume fraction of each phase and the fluid properties.

(2) The Energy Equation:-

$$\frac{\partial}{\partial t}(\rho E) + \nabla.(v(\rho E + p)) = \nabla.(k_{eff}\nabla T) + S_h \qquad \ldots\ldots\ldots\ldots(2)$$

Here E treated as mass averaged variables,and it is given by,

$$E = \frac{\sum_{q=1}^{q=n} \alpha_q \rho_q E_q}{\sum_{q=1}^{n} \alpha_q \rho_q} \quad \ldots\ldots\ldots\ldots\ldots\ldots\ldots\ldots\ldots\ldots\ldots\ldots\ldots\ldots(3)$$

For k-ε turbulent model:

$$\frac{\partial \rho k}{\partial t} + \frac{\partial \rho k u}{\partial x} = \frac{\partial}{\partial x}\left(\frac{v_t}{\sigma_k}\frac{\partial k}{\partial x} + v\frac{\partial k}{\partial x}\right) + p_k - \rho\varepsilon \quad \ldots\ldots\ldots\ldots\ldots(4)$$

$$\frac{\partial \rho \varepsilon}{\partial t} + \frac{\partial \rho \varepsilon u}{\partial x} = \frac{\partial}{\partial x}\left(\frac{v\partial \varepsilon}{\sigma \partial x}\right) + c_1 \frac{\varepsilon}{k} p_k - c_2 \rho \frac{\varepsilon^2}{k} \quad \ldots\ldots\ldots\ldots\ldots(5)$$

where the generated item of turbulent kinetic energy,

$$p_k = v_t\left[\frac{\partial u_i}{\partial x_i} + \frac{\partial u_j}{\partial u_j}\right]\frac{\partial u_i}{\partial x_j} \quad \ldots\ldots\ldots\ldots\ldots\ldots\ldots\ldots\ldots\ldots\ldots\ldots...(6)$$

the turbulent viscous coefficient $v_t = \frac{\rho c_\mu k^2}{\varepsilon}$ and the constant value:

C_1=1.44,C_2=1.92,σ_z=1.0,σ_ε=1.3,C_μ=.09

3.1.2 Boundary conditions:

Pressure inlet boundary at top face was used to define the pressure at inlet along with all other scalar properties of flow, and all other faces i.e. left, right, front, rear and bottom part of the cube was set as wall. In wall boundary condition stationary wall was selected as wall motion and in shear condition no slip was chosen. The no slip condition indicates the fluid sticks to the wall and moves with same velocity of wall, if it is moving.

3.1.3 Grid employed:

A body fitted hexagonal grid has been taken as shown in the figures. The type of meshing scheme was cooper type in cooper meshing scheme. GAMBIT treats the volume as consisting of one or more logical cylinders each of which is composed of two end caps and a barrel. Faces that include the caps of such cylinders are called “source” faces; while the other cylinders are called “non-source” faces. Finally interval size of the grid was set to a value such that it the liquid drop is defined in a minimum of 8 grids.

3.1.4 Residual and convergence:

Residuals are used for checking convergence of the solution. Here scale residual has been because it is a more appropriate indicator of convergence of this type of problem. FLUENT scales the residual using a scaling factor which represent the flow rate of a general variable through the domain. In this study a fixed value of 0.00001 has been selected for the absolute criteria of continuity, *x*- velocity, *y*-velocity, *z*-velocity and energy, owing to the smaller volumes involved. A detailed step by step procedure of implementation is described below:

3.2: Procedure to define a UDF controlled solution:

Step 1: A cuboid model of dimensions 12mm(x) by 12mm(y) by 7mm(z) is created by stitching its six faces as shown below:

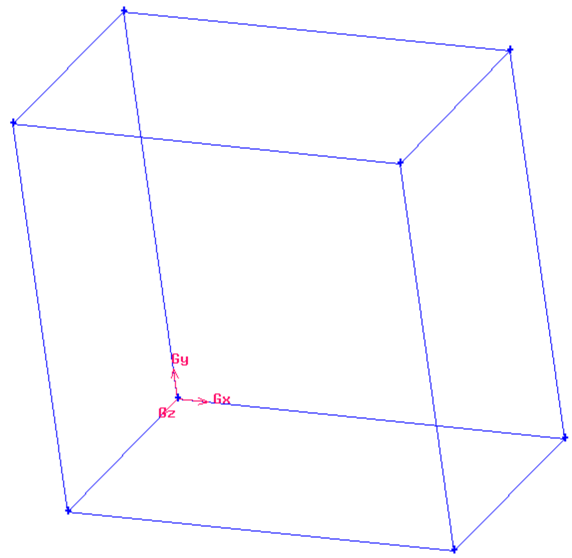

Step 2: For the analysis of a drop of $10mm^3$, a mesh size of 0.1875mm is suffice to contain 18 grids in the diameter. Hence the model has been meshed using hexagon cooper type mesh with the above mesh size and the faces are named as top, bottom, right, left, front and rear as shown below:

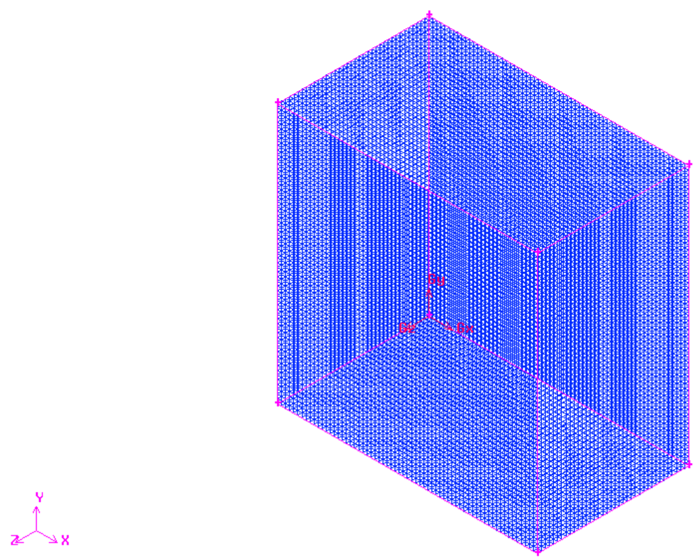

Step 3: The above mesh file was imported to fluent and an unsteady solver has been adopted as shown:

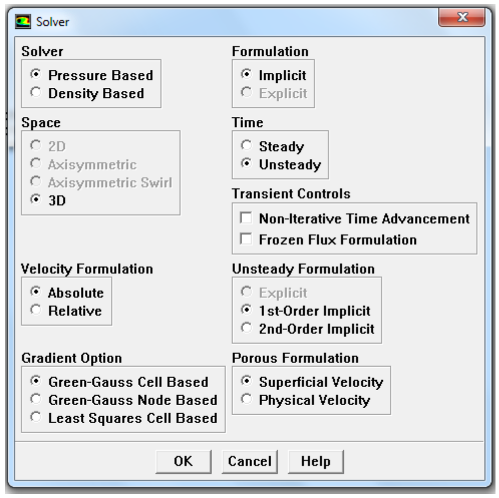

Step 4: Material properties and operating conditions have been defined with gravity, its direction (-z axis) and operating density of the drop as shown below:

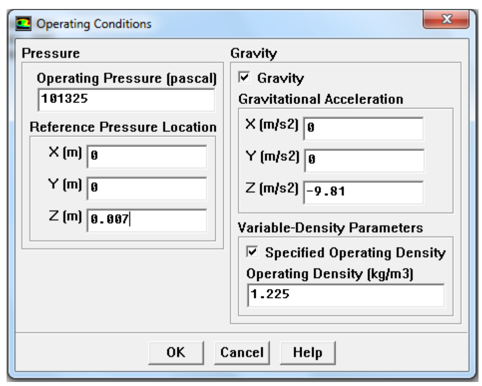

Step 5: The UDF source code (coded in an editor) was invoked and interpreted using the interpreter as shown below (content of UDF on right side):

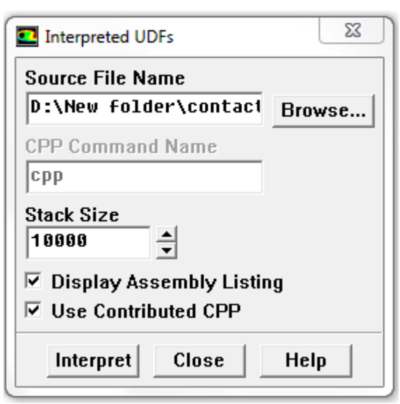

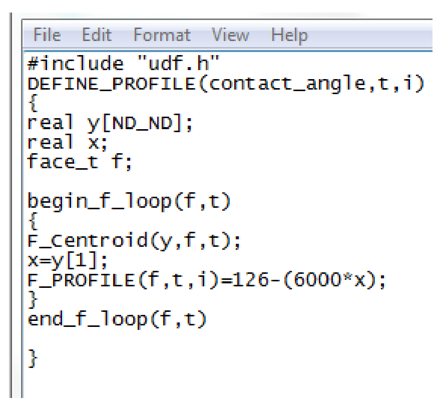

Step 6: The configuration file generated was hooked to the bottom face in boundary condition panel to define the contact angle values at each node:

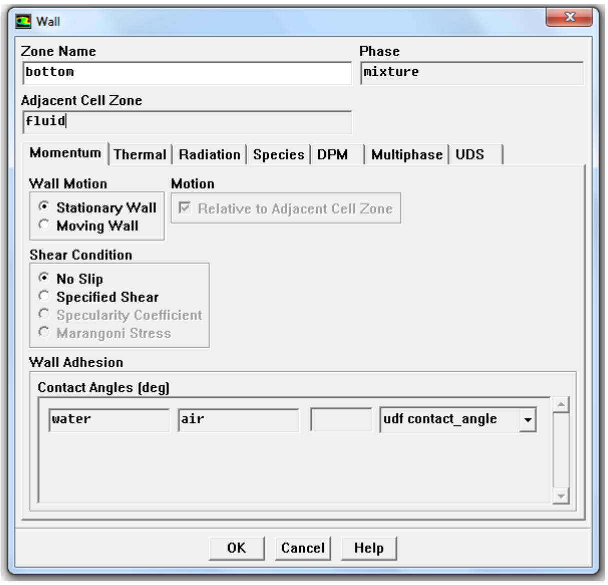

Step 7: The PISO solver was adopted for solution with all under-relaxation factors being set to 1:

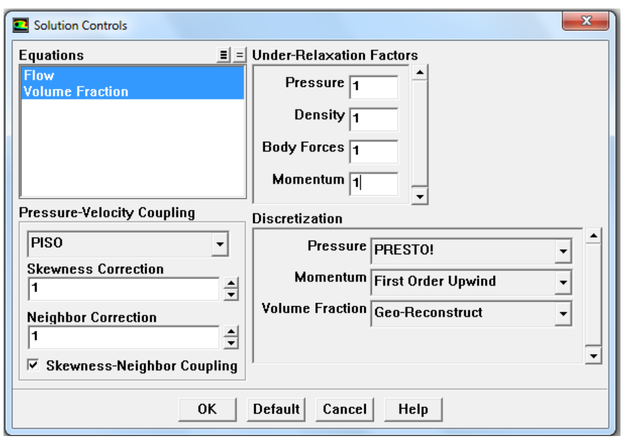

Step 8: The solution was initialized and the region containing the drop (initial position) was marked and then patched assuming an initial hemispherical shape of the droplet:

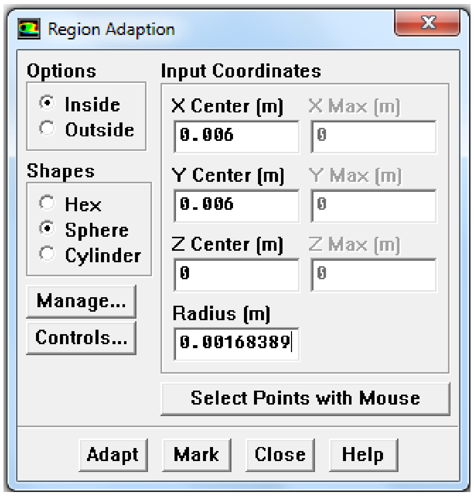

Step 9: A plane was defined passing through the mid-section of x-y plane and along which the drop was supposed to move, to have a visual aspect of the movement w.r.t. time along its transverse section and the initial position of the drop.

Step 10: The initial data was saved and iteration was processed till the final position of the drop after a predefined time period was obtained. The residual results have been plotted as shown below:

The above method was followed during formulation of each solution obtained. Initially a specific volume was taken and a wettability gradient was established over the base surface (bottom). Depending upon the movement of the drop, the wettability gradient was increased or decreased and made to iterate again until the state was reached when the drop just starts to propel itself, denoting the critical wettability gradient. The process was repeated so as to contain volumes ranging from 1mm^3 to 50mm^3 and a graph was plotted.

In the analysis of the first phase, steps 1 to 10 remain same except step 5 was omitted and the contact angle values at the boundary conditions panel was defined constant values, as depicted in results.

Chapter 4

4. RESULTS OBTAINED:

The analysis of the first phase of results as depicted above yielded the following results as could be observed over time steps below:

(i) Water Drop over steel surface with a contact angle of 90^0 between them: A fixed volume hemispherical model has been developed as an initial approximation of the shape and the contact angle was specified a constant value. Under the influence of external forces including gravity, the model has been iterated over 3000 time steps with step size of 0.0001s and results have been recorded after every 50 time steps. The shapes acquired by the drop over different time steps are shown in Figure 3 below:

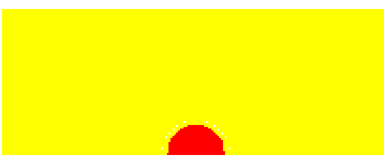
t=0.000 sec

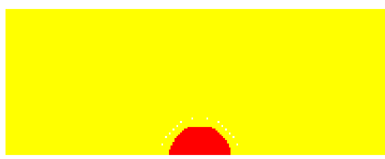
t=0.005 sec

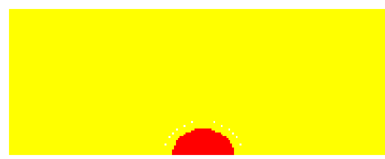
t=0.010 sec

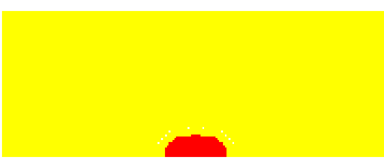
t=0.015 sec

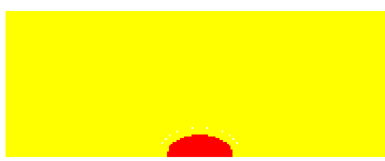
t=0.020 sec

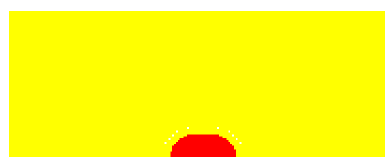
t=0.025 sec

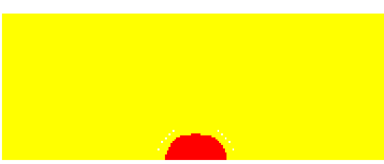
t=0.030 sec

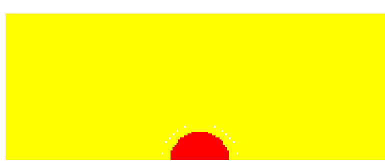
t=0.035 sec

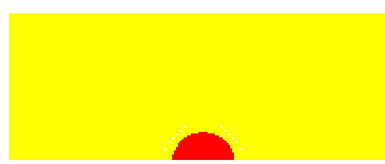
t=0.040 sec

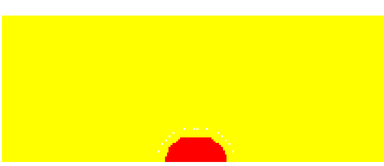
t=0.045 sec

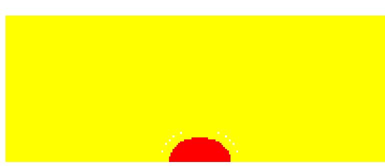
t=0.050 sec

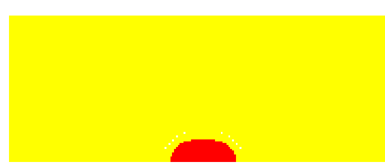
t=0.055 sec

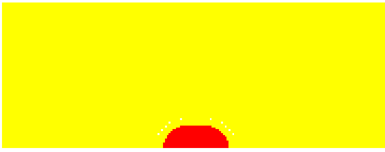
t=0.060 sec

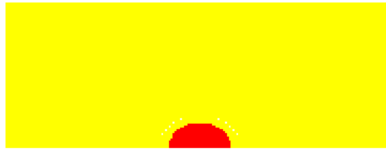
t=0.065 sec

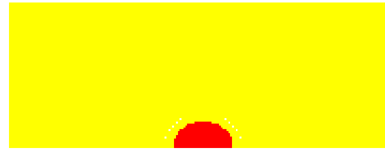
t=0.070 sec

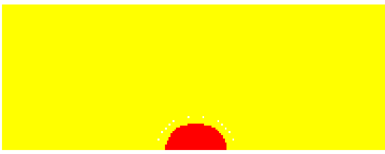
t=0.075 sec

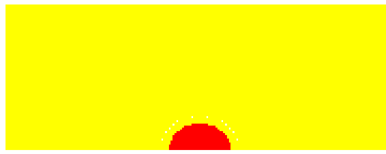
t=0.080 sec

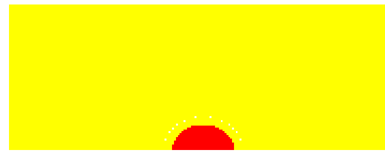
t=0.085 sec

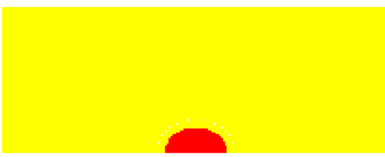
t=0.090 sec

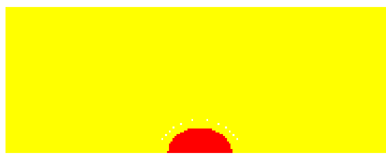
t=0.095 sec

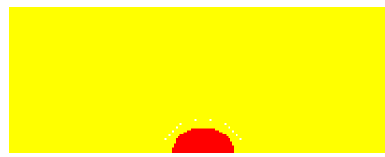
t=0.100 sec

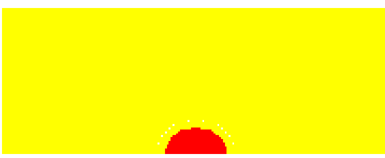
t=0.105 sec

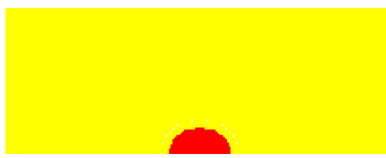
t=0.110 sec

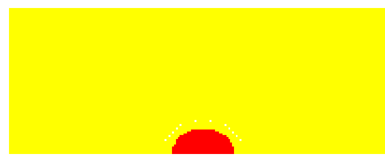
t=0.115 sec

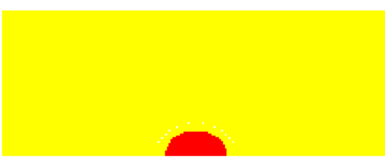
t=0.120 sec

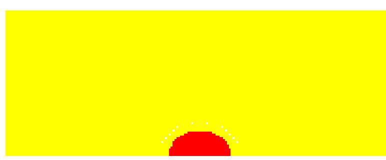
t=0.125 sec

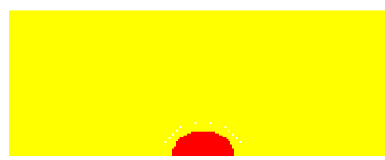
t=0.130 sec

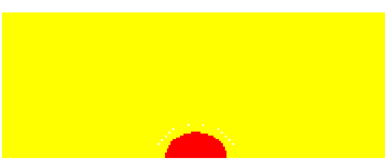
t=0.135 sec

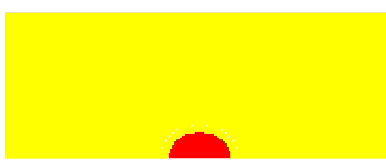
t=0.140 sec

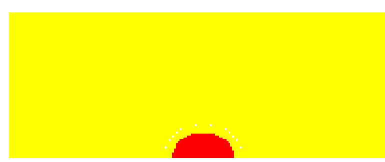
t=0.145 sec

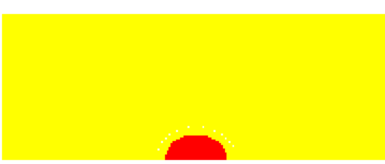
t=0.150 sec

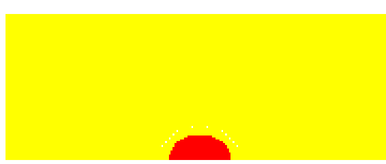
t=0.155 sec

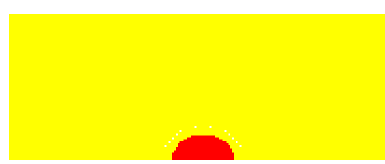
t=0.160 sec

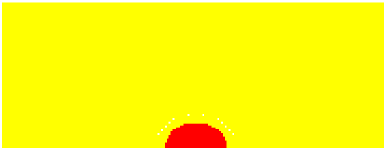
t=0.165 sec

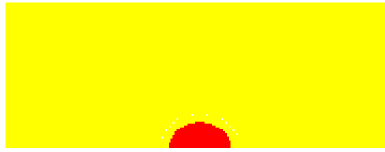
t=0.170 sec

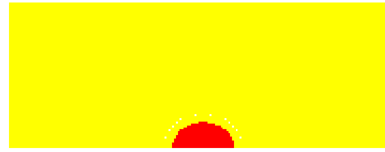
t=0.175 sec

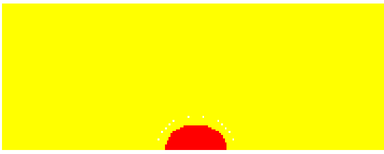
t=0.180 sec

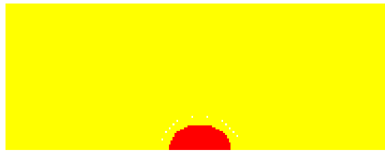
t=0.185 sec

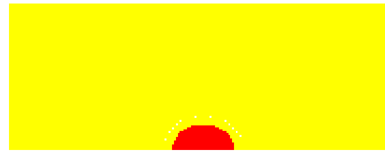
t=0.190 sec

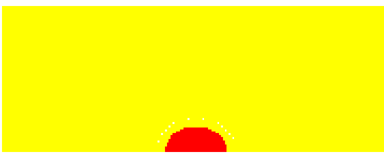
t=0.195 sec

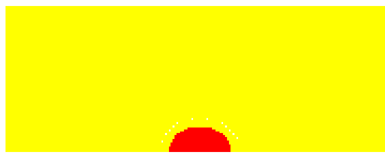
t=0.200 sec

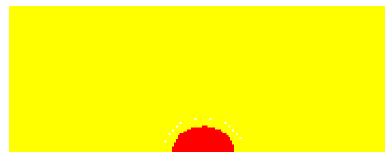
t=0.205 sec

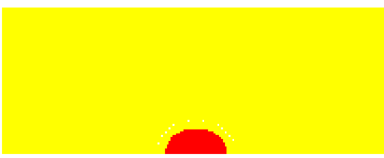
t=0.210 sec

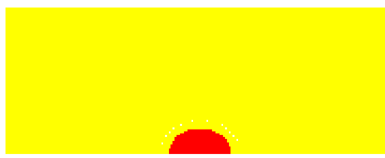
t=0.215 sec

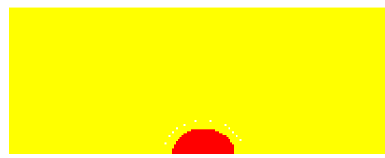
t=0.220 sec

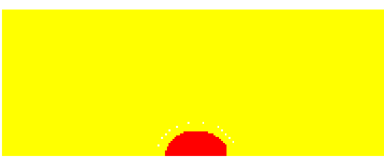
t=0.225 sec

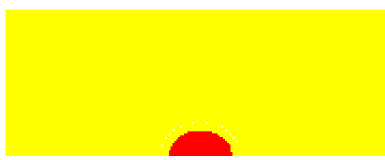
t=0.230 sec

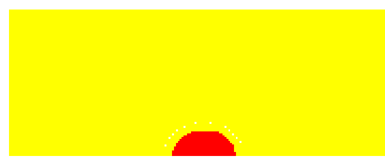
t=0.235 sec

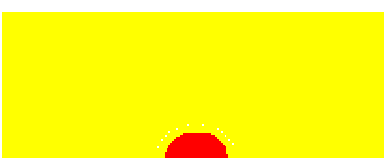
t=0.240 sec


t=0.245 sec

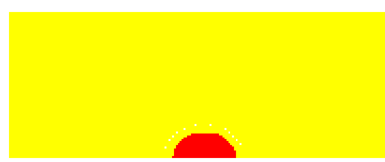
t=0.250 sec

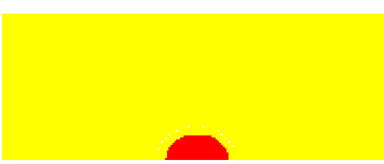
t=0.255 sec

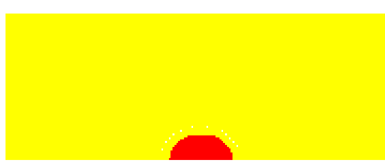
t=0.260 sec

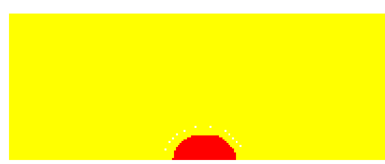
t=0.265 sec

t=0.300 sec

Figure 3: Equilibrium shapes of drop over a horizontal plane with contact angle of 90^0.

Also the contours of velocity plots over the surface of the drop has been obtained over different time steps as shown in Figure 4 below:

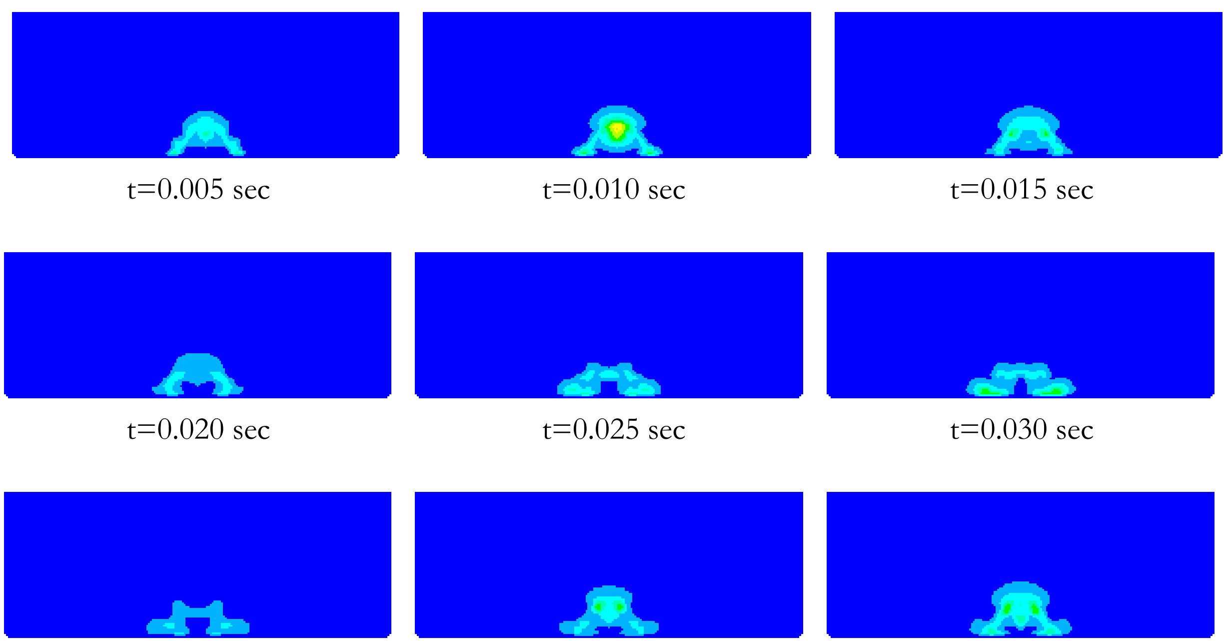

t=0.045 sec

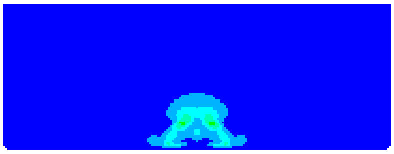
t=0.050 sec

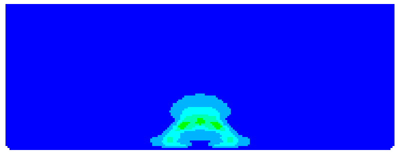
t=0.055 sec

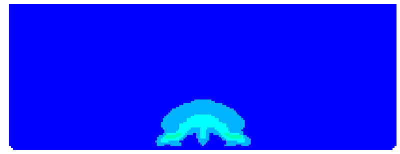
t=0.060 sec

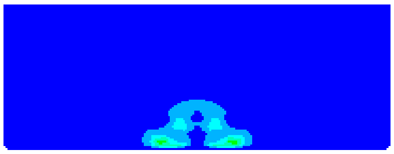
t=0.065 sec

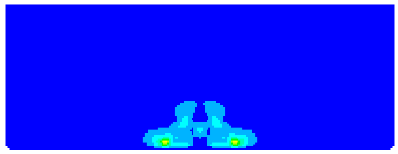
t=0.070 sec

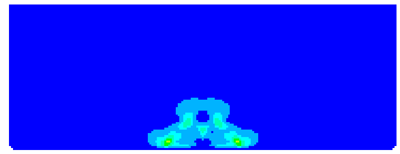
t=0.075 sec

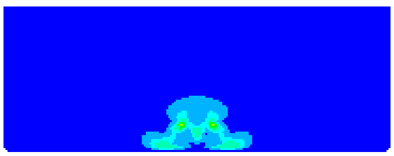
t=0.080 sec

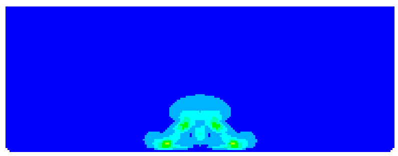
t=0.085 sec

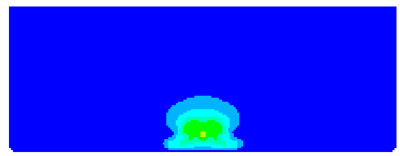
t=0.090 sec

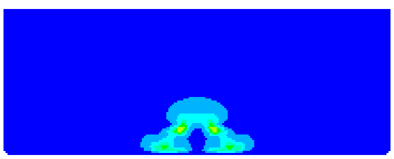
t=0.095 sec

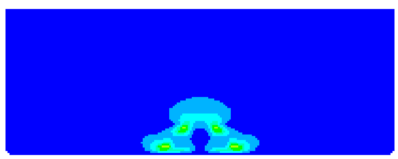
t=0.100 sec

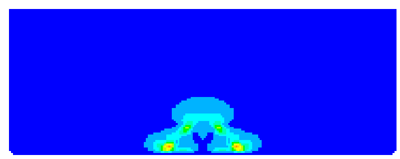
t=0.105 sec

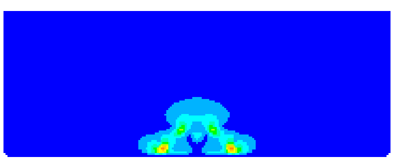
t=0.110 sec

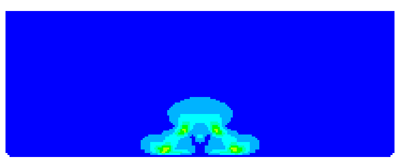
t=0.115 sec

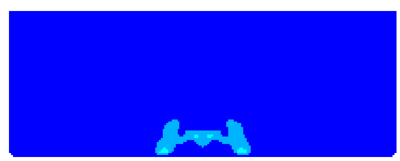
t=0.120 sec

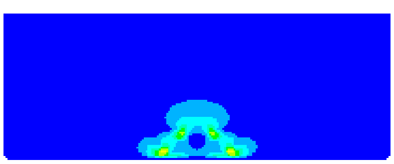
t=0.125 sec

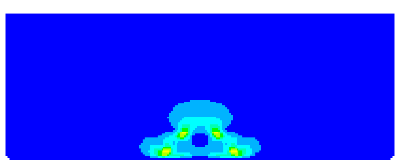
t=0.130 sec

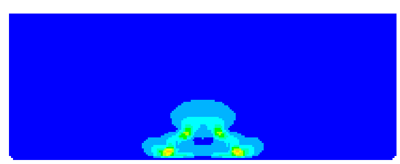
t=0.135 sec

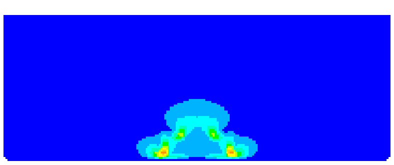
t=0.140 sec

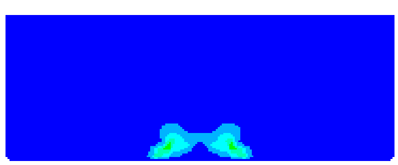
t=0.145 sec

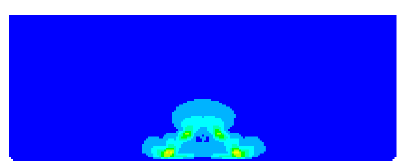
t=0.150 sec

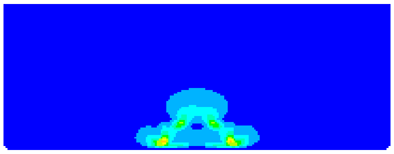
t=0.155 sec

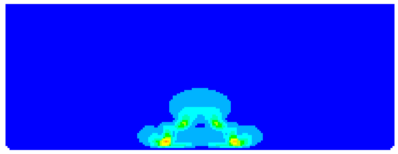
t=0.160 sec

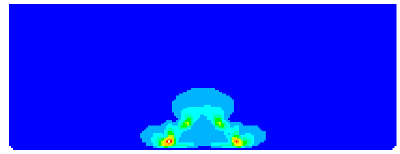
t=0.165 sec

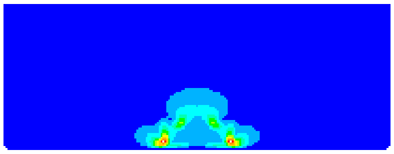
t=0.170 sec

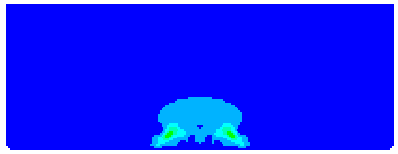
t=0.175 sec

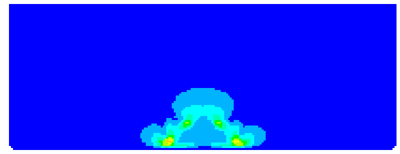
t=0.180 sec

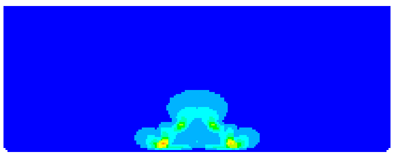
t=0.185 sec

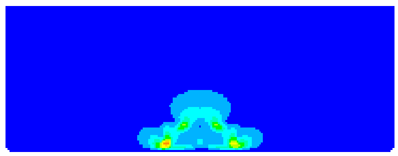
t=0.190 sec

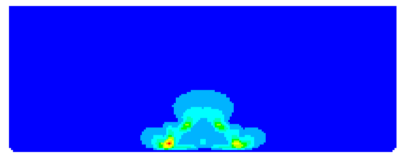
t=0.195 sec

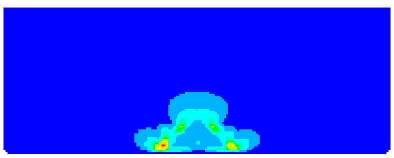
t=0.200 sec

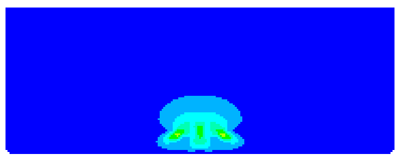
t=0.205 sec

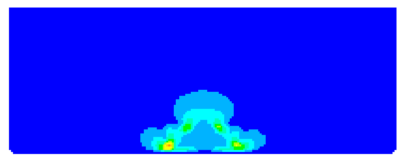
t=0.210 sec

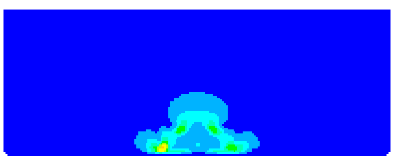
t=0.215 sec

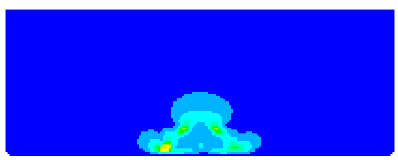
t=0.220 sec

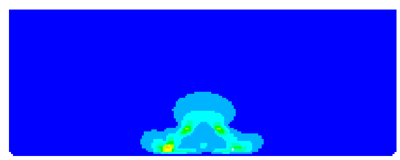
t=0.225 sec

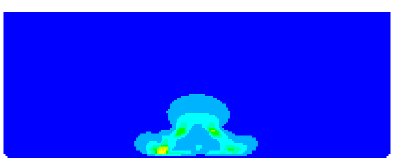
t=0.230 sec

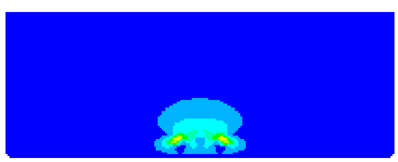
t=0.235 sec

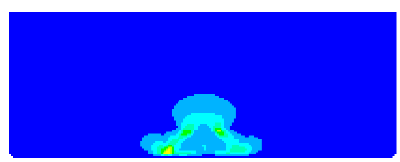
t=0.240 sec

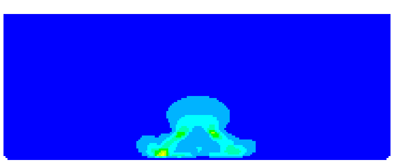
t=0.245 sec

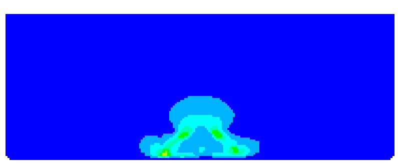
t=0.250 sec

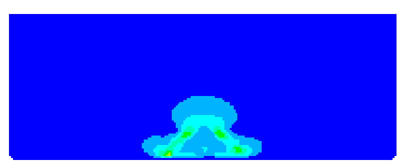
t=0.255 sec

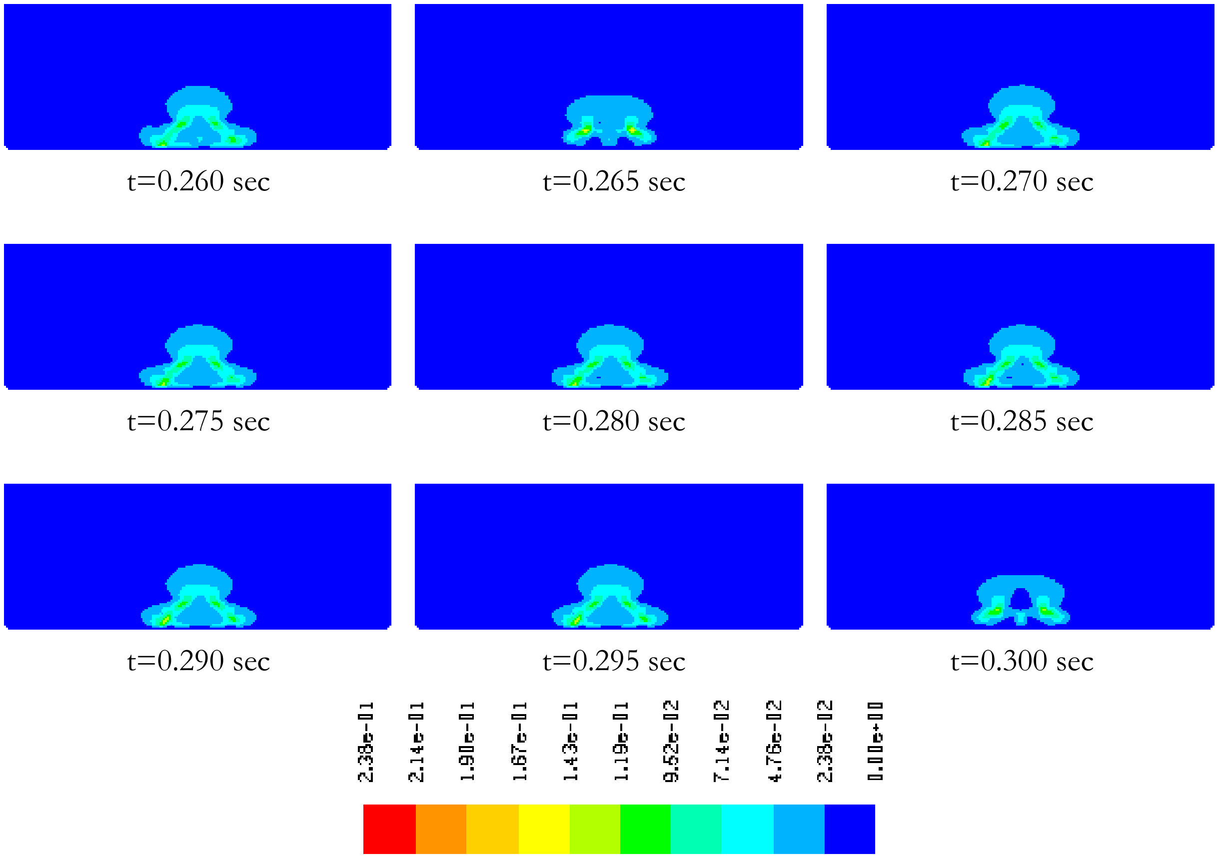

Figure 4: Velocity contours of drop over a horizontal plane with contact angle of 90^0.

(ii)Water Drop over solid surface with a contact angle of 60^0 between them: As earlier, a fixed volume hemispherical model has been developed and all the boundary conditions remain same except the contact angle which is constant over the circumference at 60^0. The model has been iterated for 3000 time steps with step size of 0.0001s. The shapes acquired over different time steps are shown in Figure 5 below:

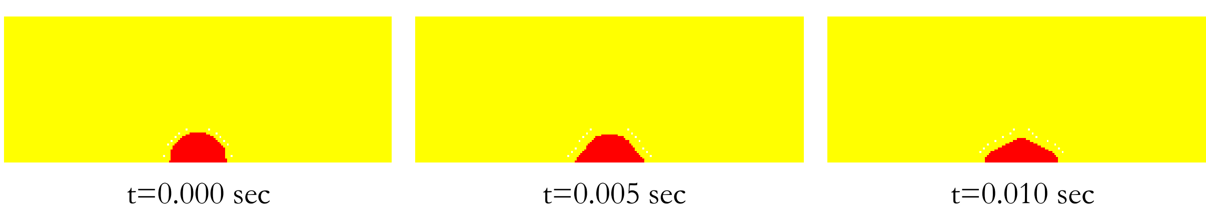

t=0.015 sec

t=0.020 sec

t=0.025 sec

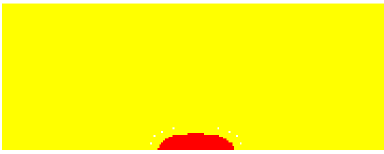
t=0.030 sec

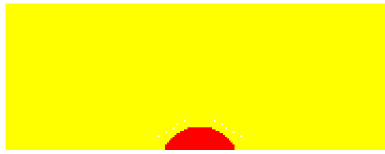
t=0.035 sec

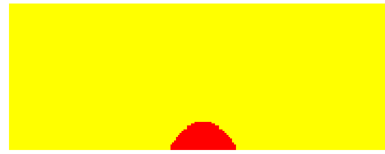
t=0.040 sec

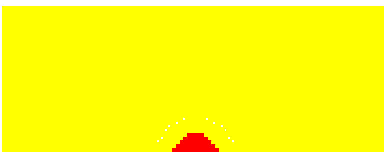
t=0.045 sec

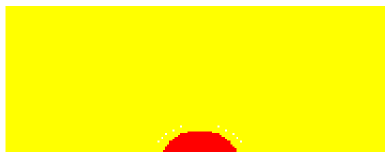
t=0.050 sec

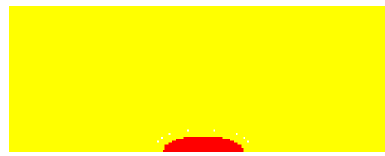
t=0.055 sec

t=0.060 sec

t=0.065 sec


t=0.070 sec

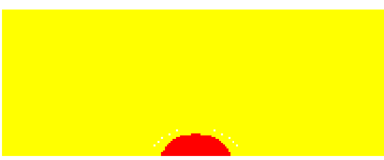
t=0.075 sec

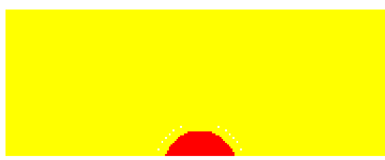
t=0.080 sec

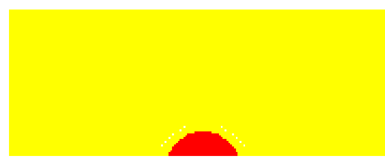
t=0.085 sec

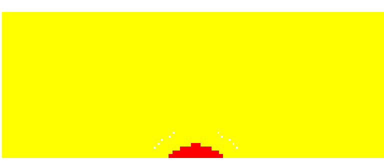
t=0.090 sec


t=0.095 sec

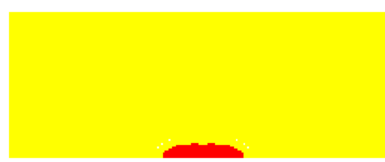
t=0.100 sec


t=0.105 sec


t=0.110 sec

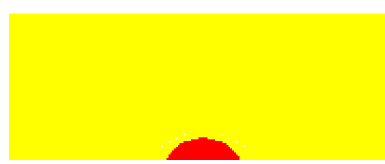
t=0.115 sec

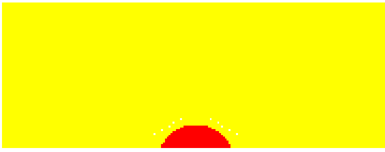
t=0.120 sec

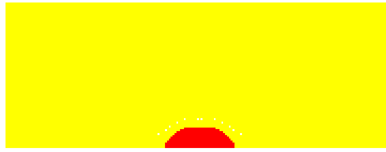
t=0.125 sec

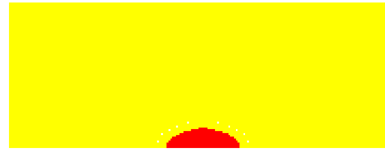
t=0.130 sec

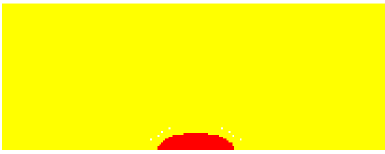
t=0.135 sec

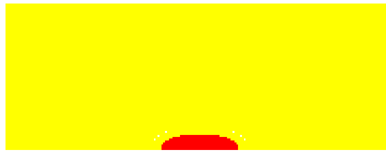
t=0.140 sec

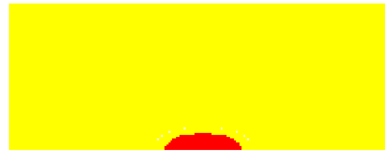
t=0.145 sec

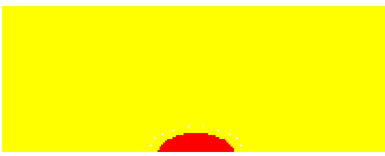
t=0.150 sec

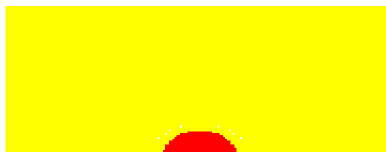
t=0.155 sec

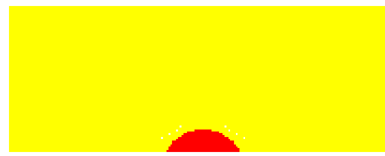
t=0.160 sec

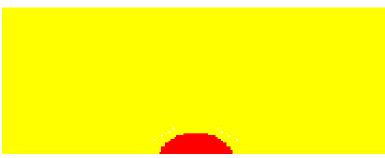
t=0.165 sec

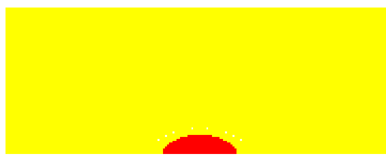
t=0.170 sec


t=0.175 sec

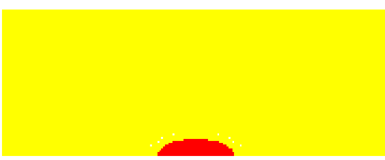
t=0.180 sec


t=0.185 sec

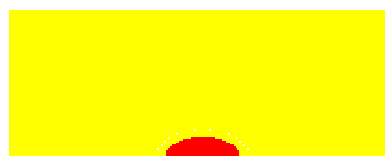
t=0.190 sec

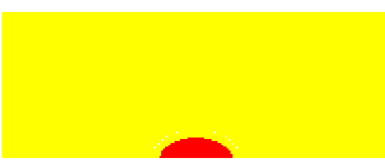
t=0.195 sec

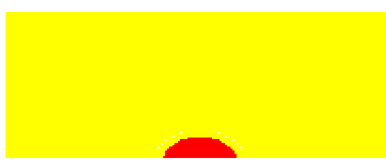
t=0.200 sec


t=0.205 sec

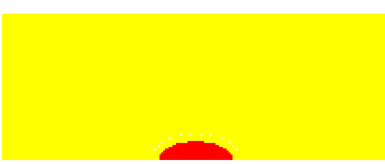
t=0.210 sec


t=0.215 sec


t=0.220 sec

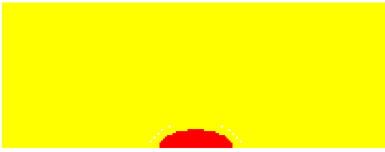
t=0.225 sec

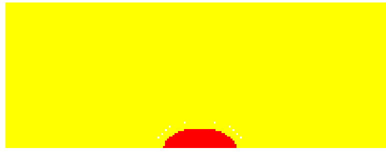
t=0.230 sec

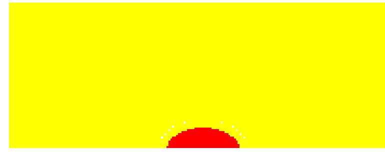
t=0.235 sec

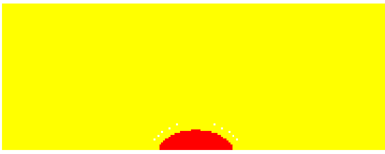
t=0.240 sec

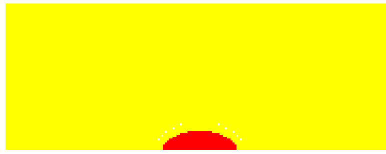
t=0.245 sec


t=0.250 sec

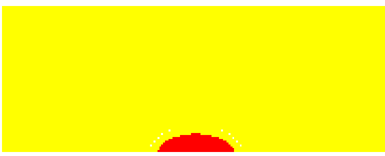
t=0.255 sec


t=0.260 sec

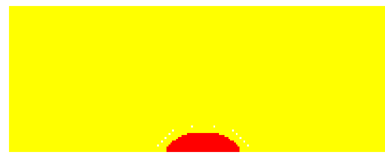
t=0.265 sec

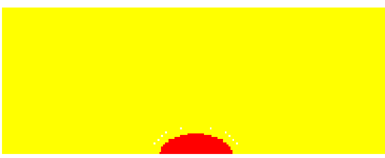
t=0.270 sec

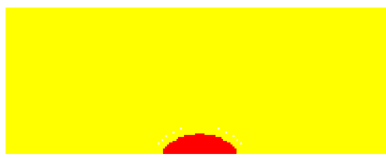
t=0.275 sec

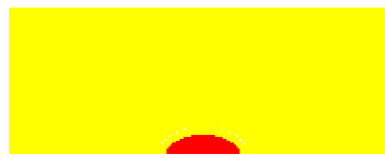
t=0.280 sec

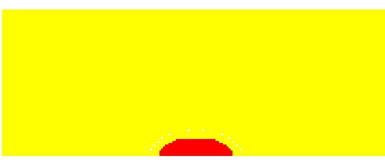
t=0.285 sec

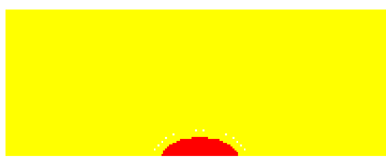
t=0.290 sec

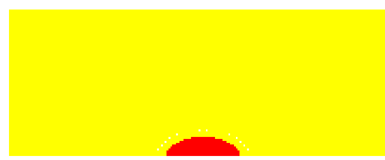
t=0.295 sec

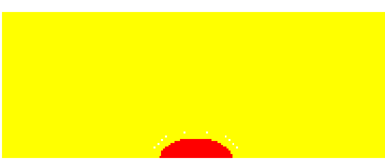
t=0.300 sec

Figure 5: Equilibrium shapes of drop over a horizontal plane with contact angle of 60^0.

The corresponding contours of velocity are plotted as in Figure 5 below:

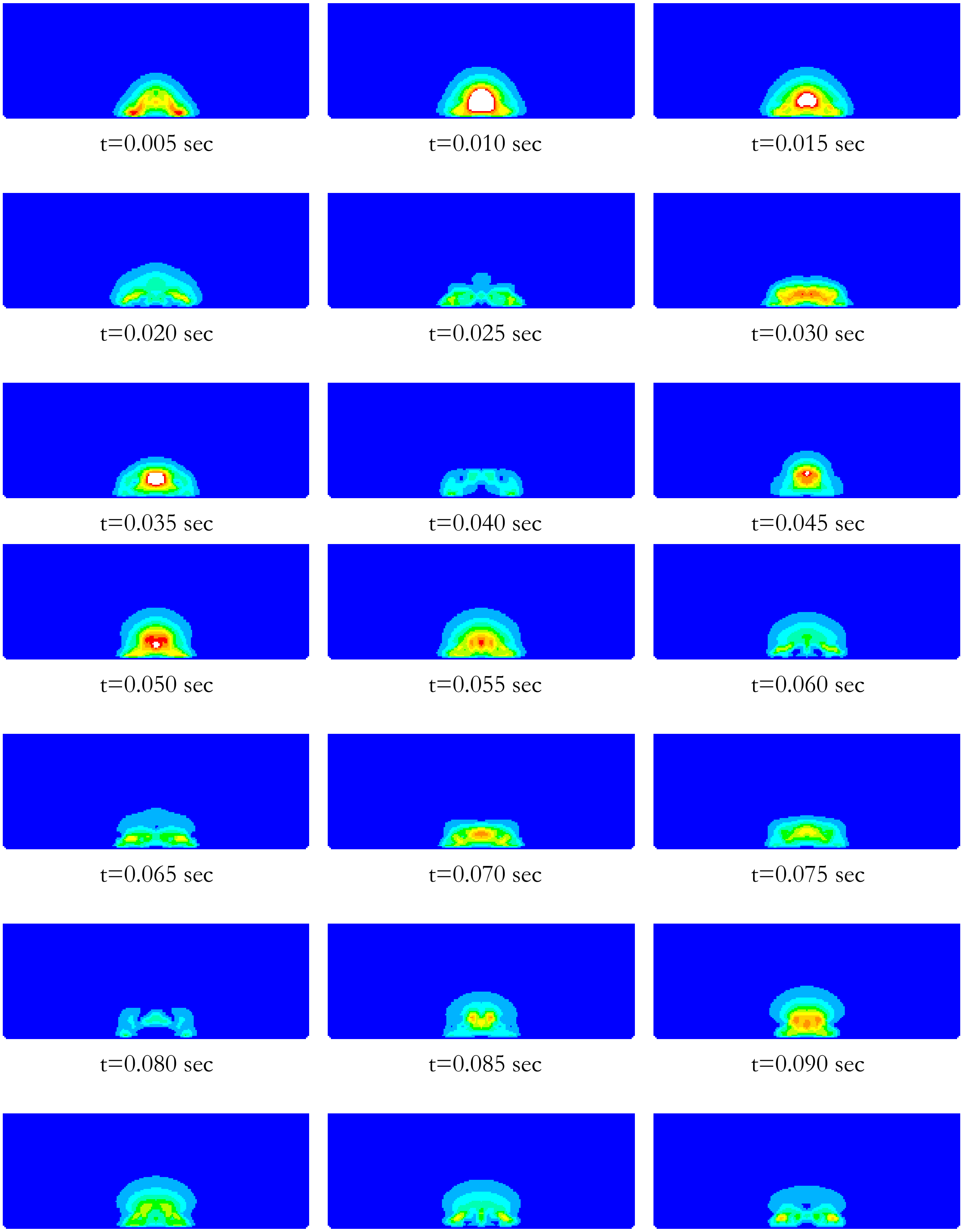

t=0.005 sec t=0.010 sec t=0.015 sec

t=0.020 sec t=0.025 sec t=0.030 sec

t=0.035 sec t=0.040 sec t=0.045 sec

t=0.050 sec t=0.055 sec t=0.060 sec

t=0.065 sec t=0.070 sec t=0.075 sec

t=0.080 sec t=0.085 sec t=0.090 sec

t=0.095 sec t=0.100 sec t=0.105 sec

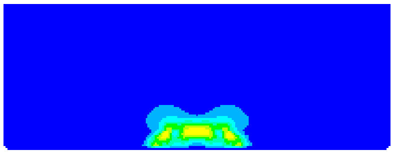
t=0.110 sec

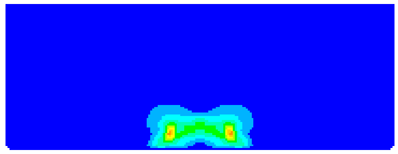
t=0.115 sec

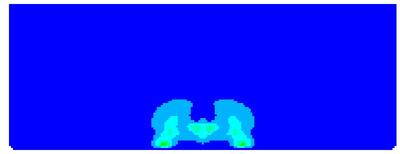
t=0.120 sec

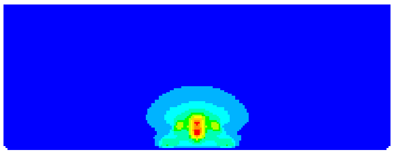
t=0.125 sec

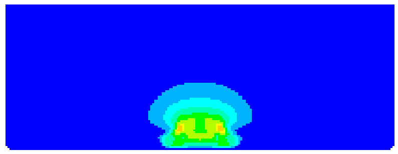
t=0.130 sec

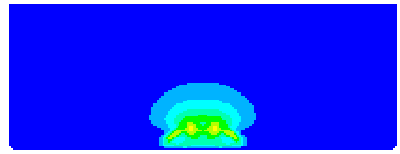
t=0.135 sec

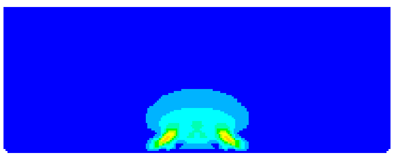
t=0.140 sec

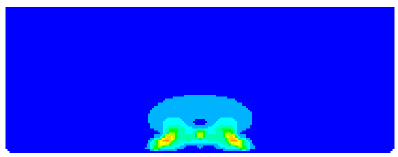
t=0.145 sec

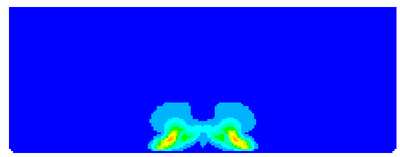
t=0.150 sec

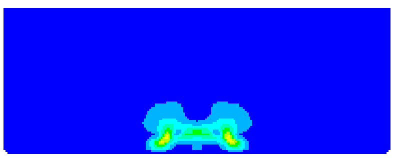
t=0.155 sec

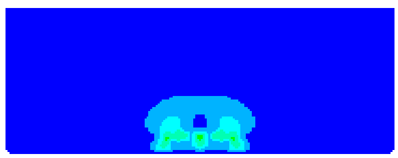
t=0.160 sec

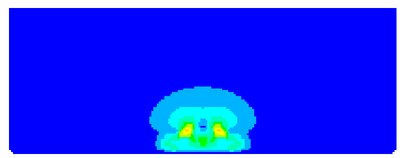
t=0.165 sec

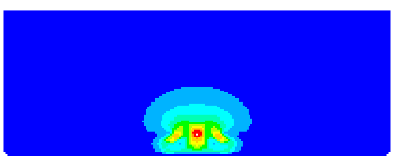
t=0.170 sec

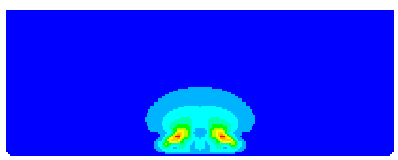
t=0.175 sec

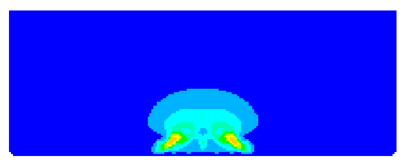
t=0.180 sec

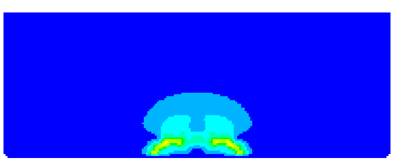
t=0.185 sec

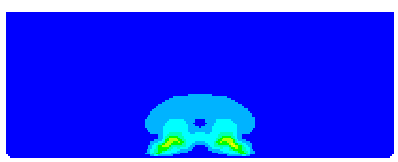
t=0.190 sec

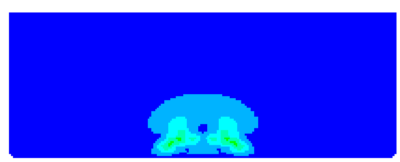
t=0.195 sec

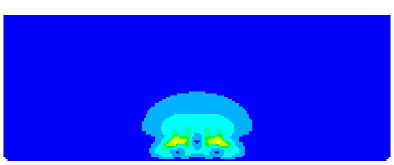
t=0.200 sec

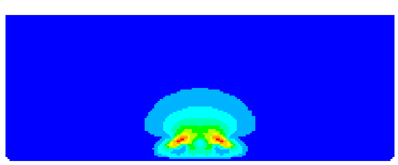
t=0.205 sec

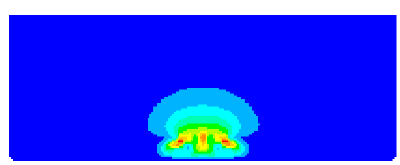
t=0.210 sec

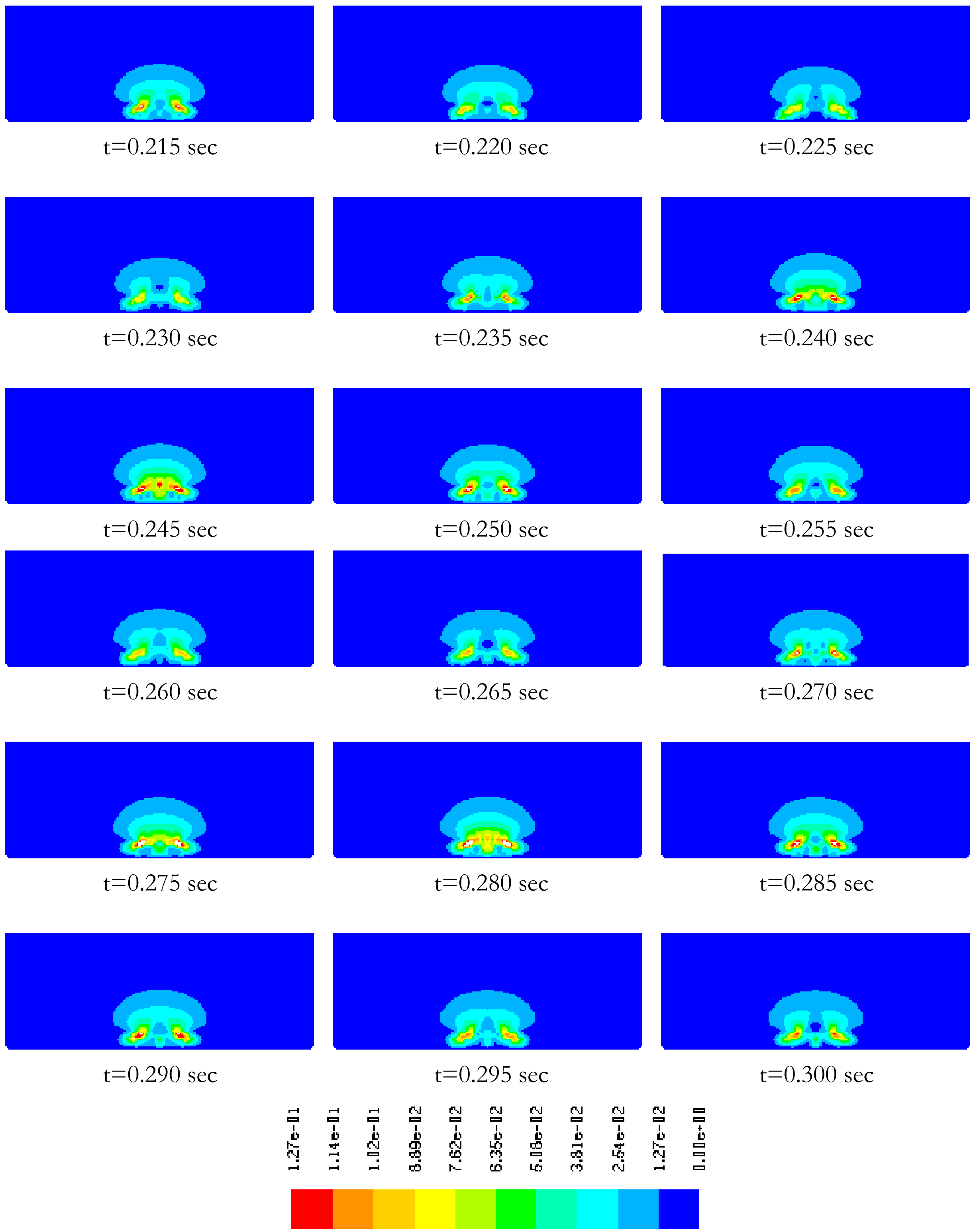

Figure 6: Velocity contours of drop over a horizontal plane with contact angle of 60^0.

(iii)Water Drop over solid surface with a contact angle of 30^0 between them: The same model was adopted but with contact angle fixed at 30^0 in the boundary conditions. Considering the same number and size of time steps, the resultant shapes acquired are shown below in Fig 7:

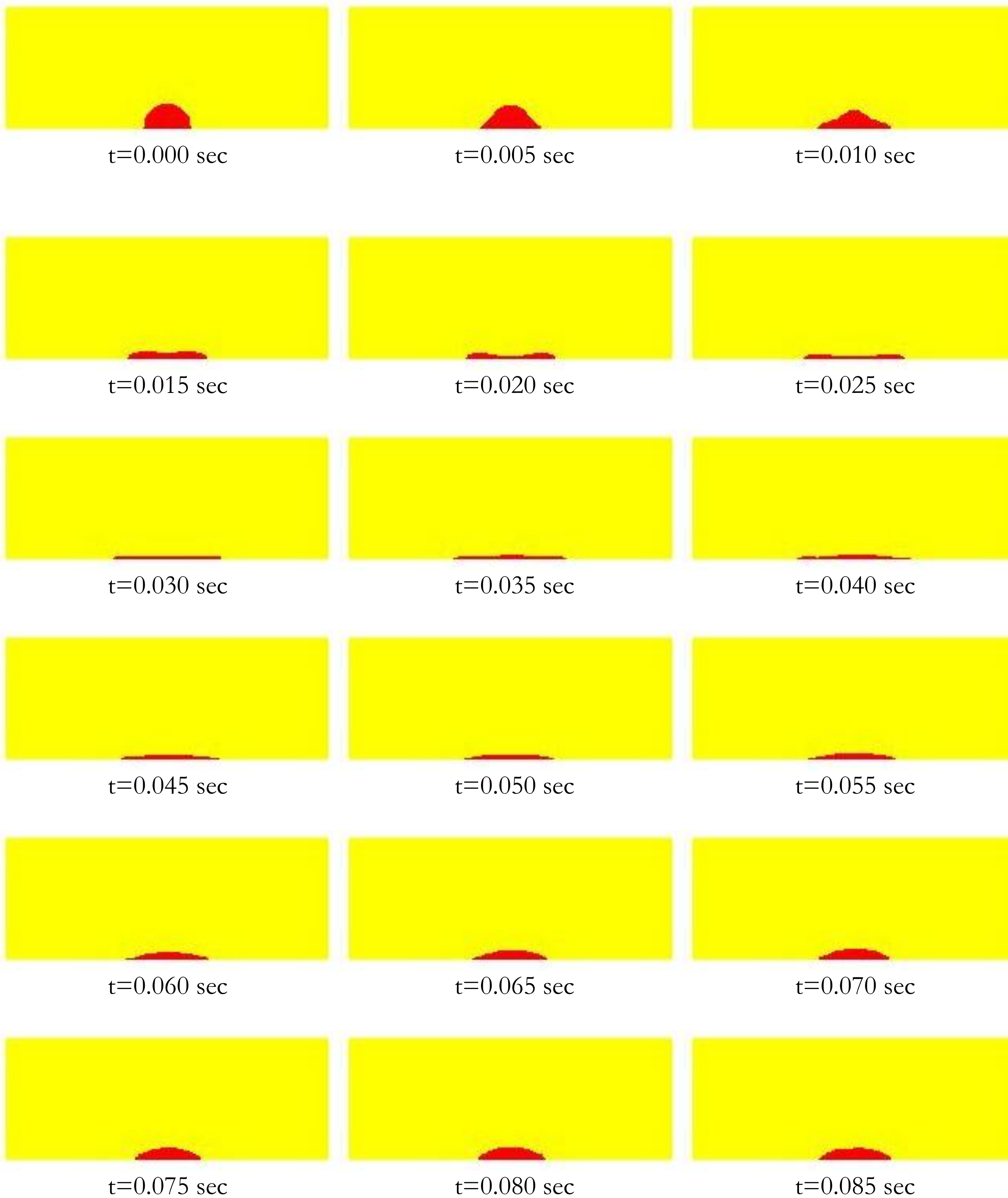


t=0.090 sec


t=0.095 sec


t=0.100 sec

t=0.105 sec

t=0.110 sec

t=0.115 sec

t=0.120 sec


t=0.125 sec

t=0.130 sec


t=0.135 sec


t=0.140 sec


t=0.145 sec


t=0.150 sec


t=0.155 sec

t=0.160 sec

t=0.165 sec

t=0.170 sec

t=0.175 sec

t=0.180 sec

t=0.185 sec

t=0.190 sec


t=0.195 sec


t=0.200 sec

t=0.205 sec

t=0.210 sec

t=0.215 sec

t=0.220 sec

t=0.225 sec

t=0.230 sec

t=0.235 sec


t=0.240 sec

t=0.245 sec


t=0.250 sec


t=0.255 sec

t=0.260 sec

t=0.265 sec

t=0.270 sec

t=0.275 sec


t=0.280 sec

t=0.285 sec

t=0.290 sec

t=0.295 sec

t=0.300 sec

Figure 7: Equilibrium shapes of water drop over a horizontal plane with contact angle of 30^0

The plots of contours of velocities at various instants are shown below in Figure 8:

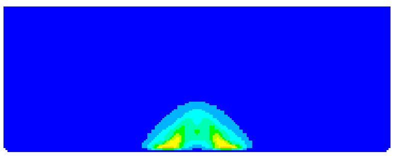

t=0.005 sec

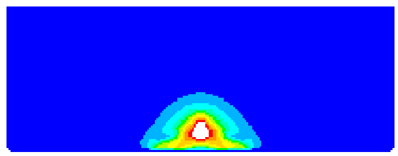

t=0.010 sec

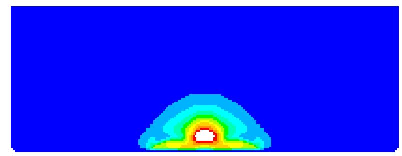

t=0.015 sec

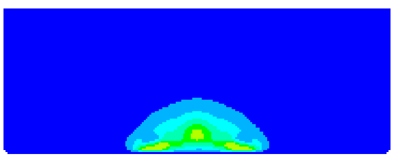

t=0.020 sec

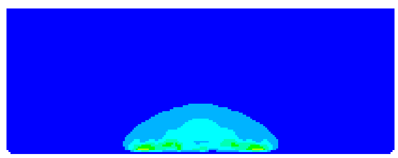

t=0.025 sec

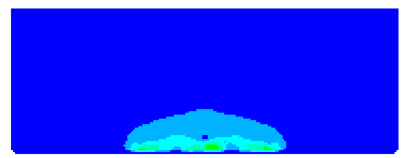

t=0.030 sec

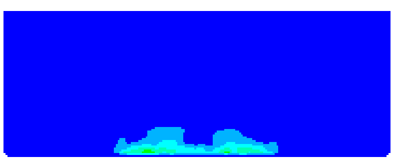

t=0.035 sec

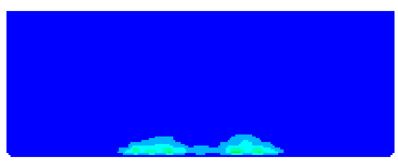

t=0.040 sec

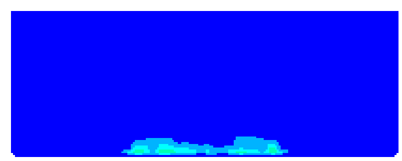

t=0.045 sec

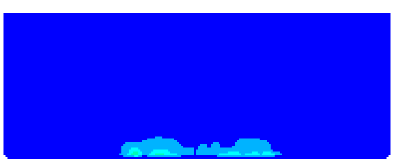

t=0.050 sec

t=0.055 sec

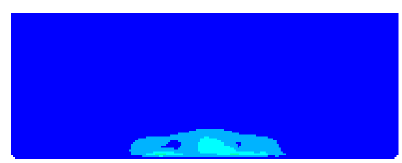

t=0.060 sec

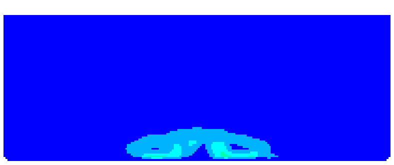

t=0.065 sec

t=0.070 sec

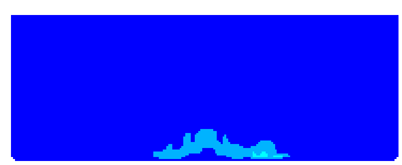

t=0.075 sec


t=0.080 sec

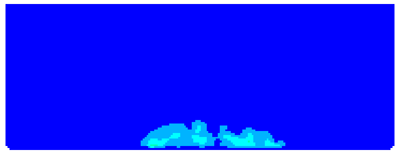
t=0.085 sec

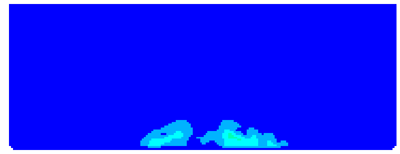
t=0.090 sec

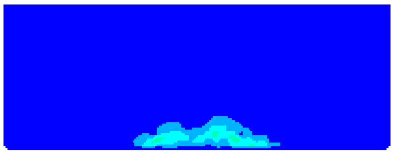
t=0.095 sec

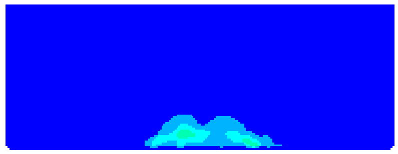
t=0.100 sec

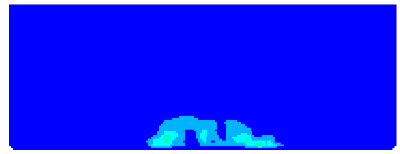
t=0.105 sec

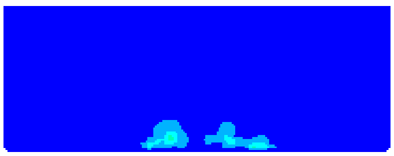
t=0.110 sec

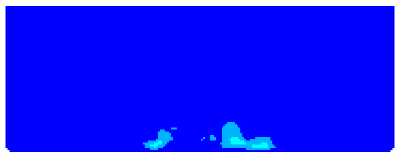
t=0.115 sec

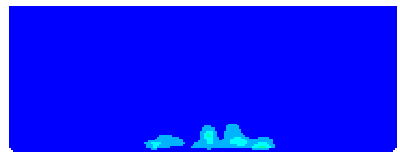
t=0.120 sec

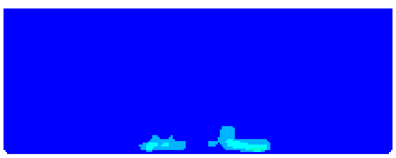
t=0.125 sec

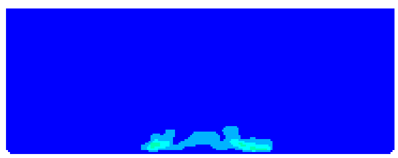
t=0.130 sec

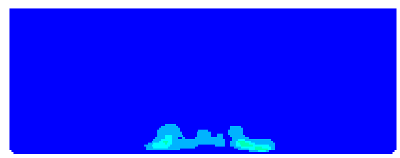
t=0.135 sec

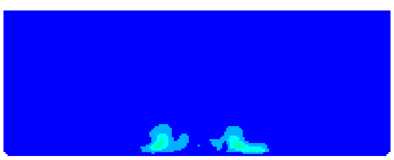
t=0.140 sec

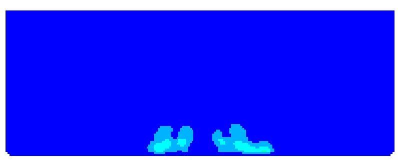
t=0.145 sec

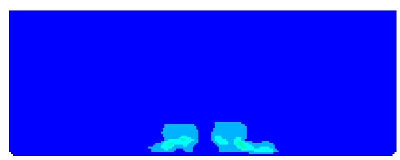
t=0.150 sec

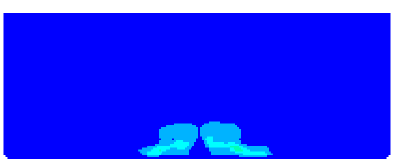
t=0.155 sec

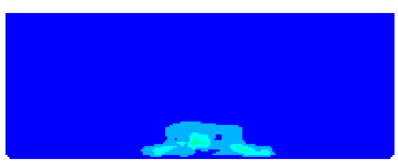
t=0.160 sec

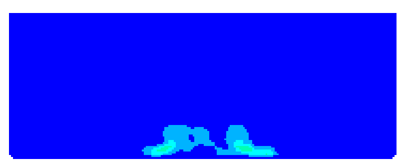
t=0.165 sec

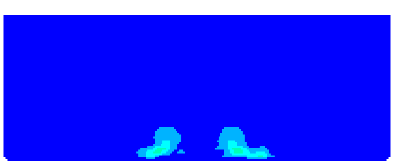
t=0.170 sec

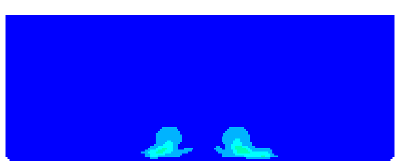
t=0.175 sec

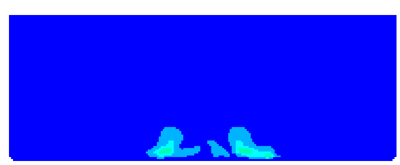
t=0.180 sec

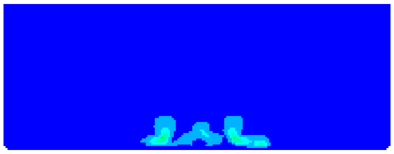
t=0.185 sec

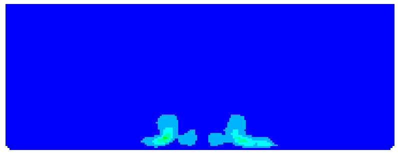
t=0.190 sec

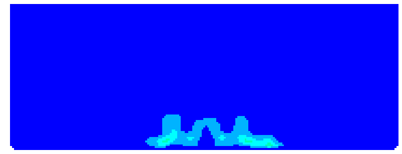
t=0.195 sec

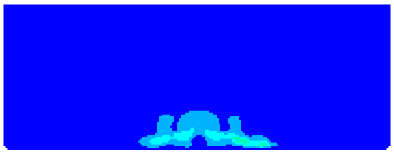
t=0.200 sec

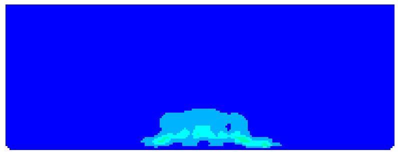
t=0.205 sec

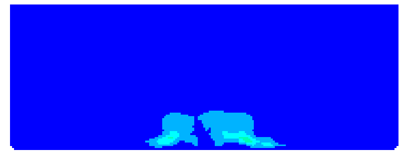
t=0.210 sec

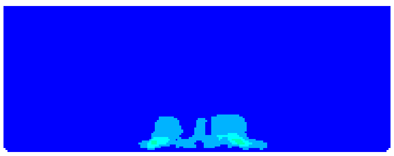
t=0.215 sec

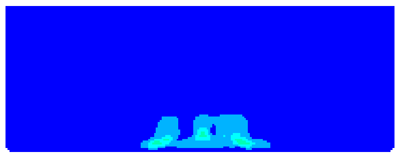
t=0.220 sec

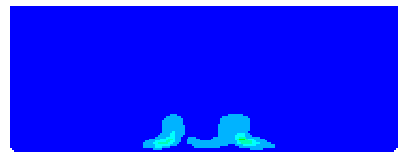
t=0.225 sec

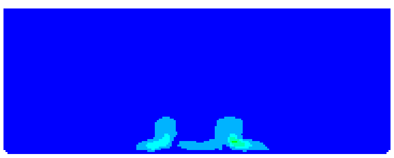
t=0.230 sec

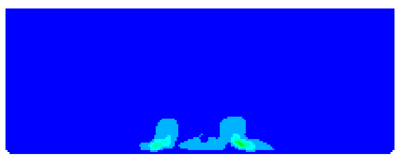
t=0.235 sec

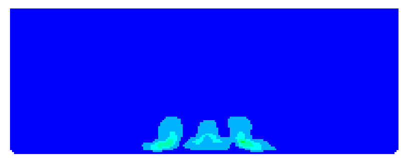
t=0.240 sec

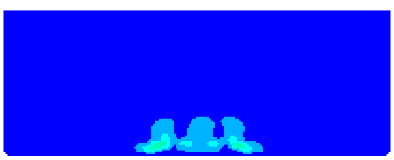
t=0.245 sec

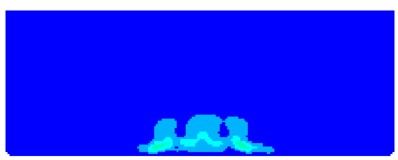
t=0.250 sec

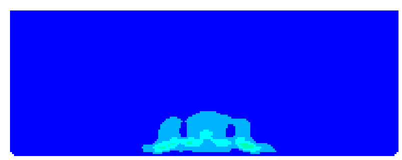
t=0.255 sec

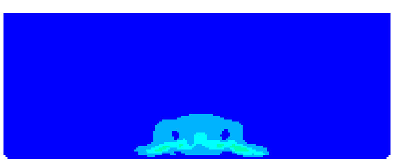
t=0.260 sec

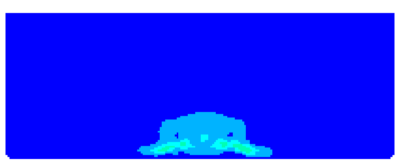
t=0.265 sec

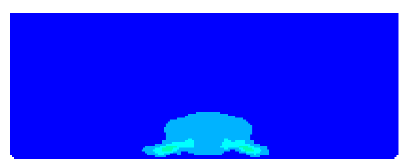
t=0.270 sec

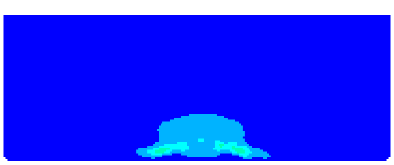
t=0.275 sec

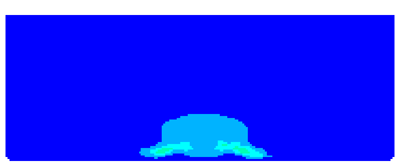
t=0.280 sec

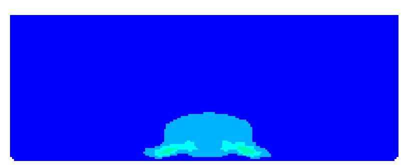
t=0.285 sec

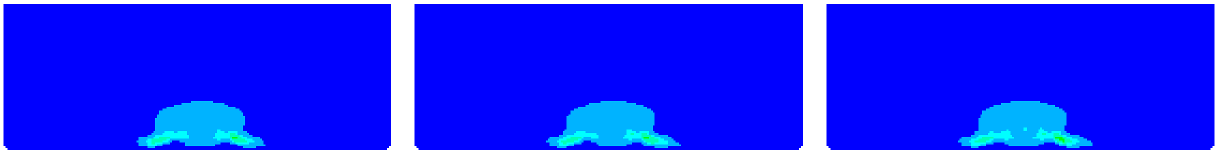

t=0.290 sec t=0.295 sec t=0.300 sec

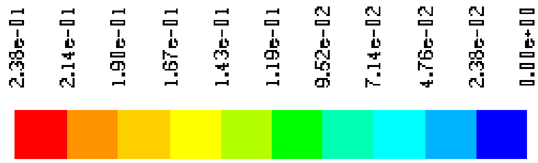

Figure 8: Velocity contours of drop over a horizontal plane with contact angle of 30^0.

(iv)Water Drop over solid surface with a contact angle of 150^0 between them: The same model has been adopted and the same numbers as well as size of time steps have been considered but contact angle has been fixed at 150^0. This case represents a less wettable combination of liquid and solid. The resultant shapes obtained by the droplet over varying intervals are represented below as Figure 8:

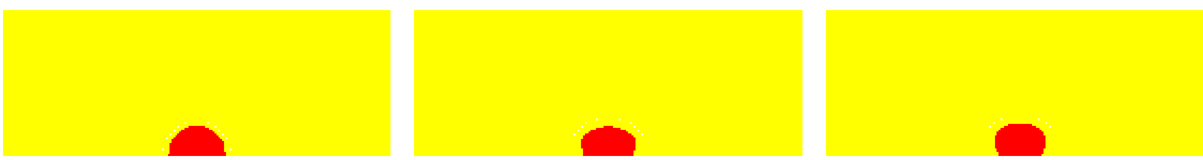

t=0.000 sec t=0.005 sec t=0.010 sec

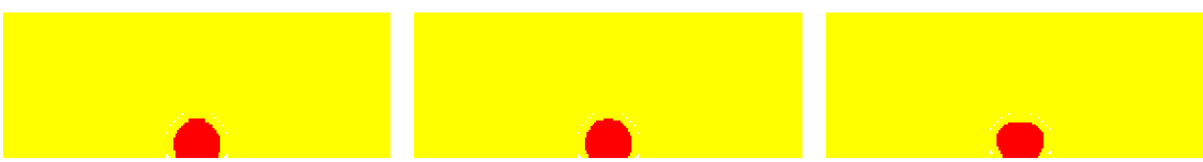

t=0.015 sec t=0.020 sec t=0.025 sec

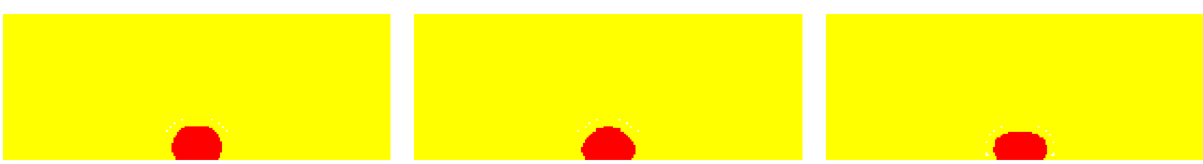

t=0.030 sec t=0.035 sec t=0.040 sec

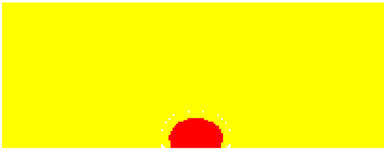
t=0.045 sec

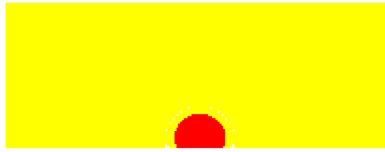
t=0.050 sec

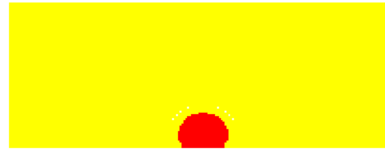
t=0.055 sec

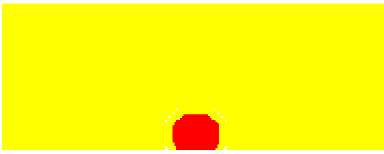
t=0.060 sec

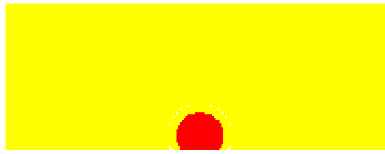
t=0.065 sec

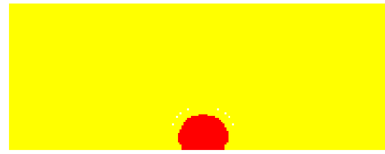
t=0.070 sec

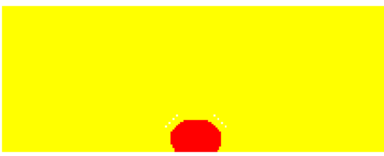
t=0.075 sec

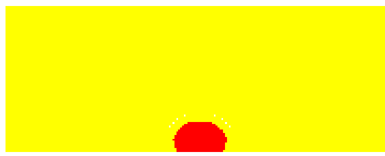
t=0.080 sec

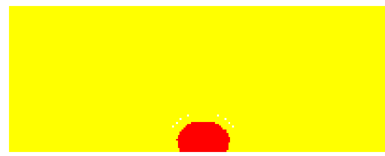
t=0.085 sec

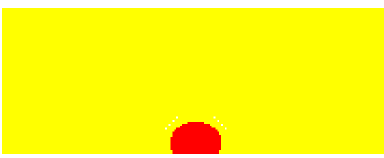
t=0.090 sec

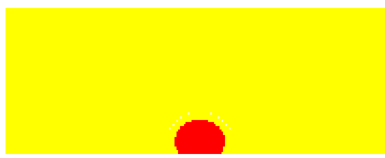
t=0.095 sec

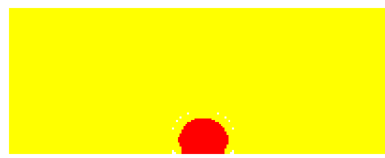
t=0.100 sec

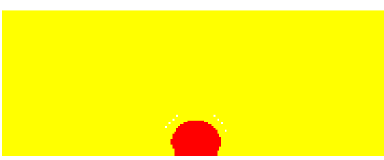
t=0.105 sec

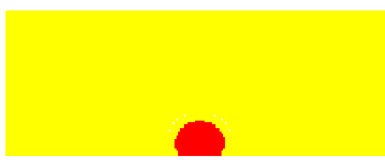
t=0.110 sec

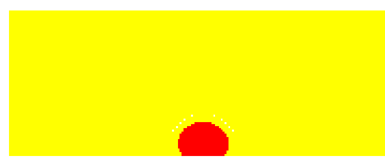
t=0.115 sec

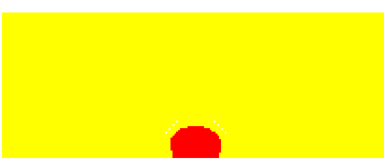
t=0.120 sec

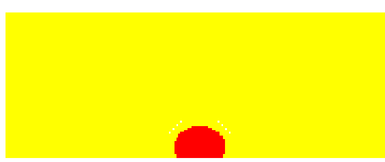
t=0.125 sec

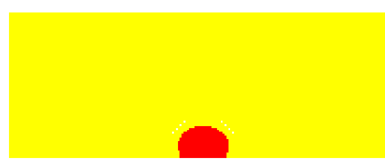
t=0.130 sec

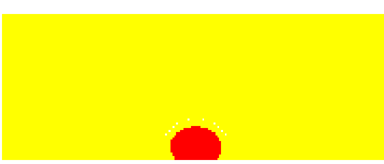
t=0.135 sec

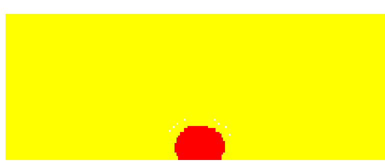
t=0.140 sec

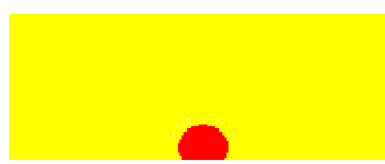
t=0.145 sec

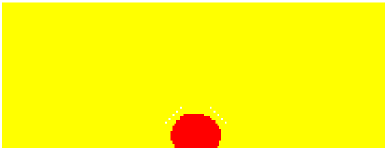
t=0.150 sec

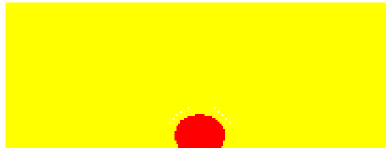
t=0.155 sec

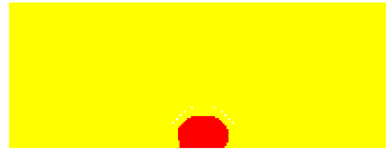
t=0.160 sec

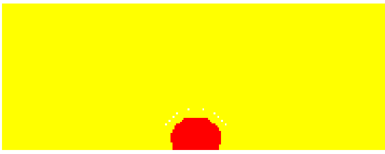
t=0.165 sec

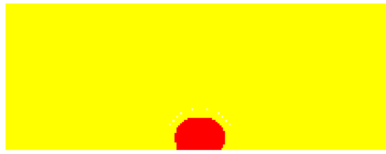
t=0.170 sec

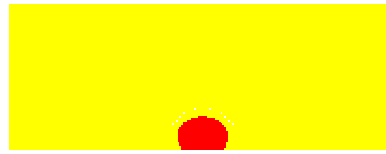
t=0.175 sec

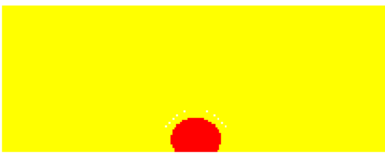
t=0.180 sec

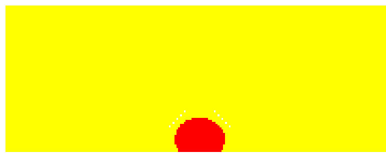
t=0.185 sec

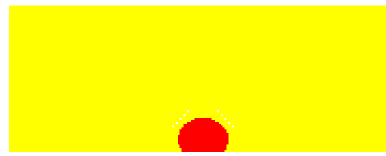
t=0.190 sec

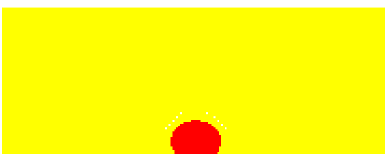
t=0.195 sec

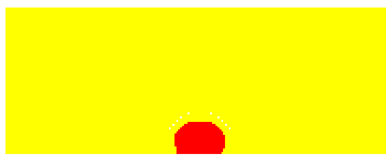
t=0.200 sec

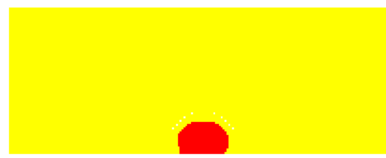
t=0.205 sec

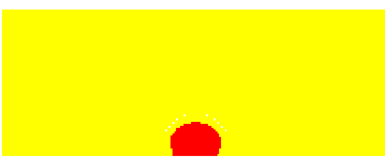
t=0.210 sec

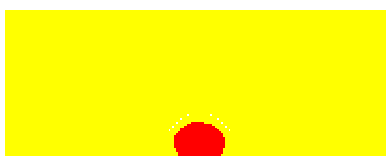
t=0.215 sec

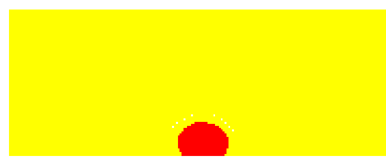
t=0.220 sec

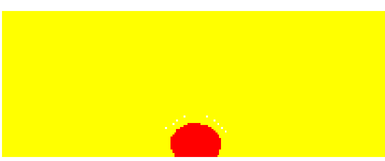
t=0.225 sec

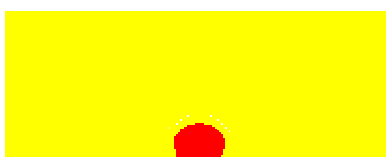
t=0.230 sec

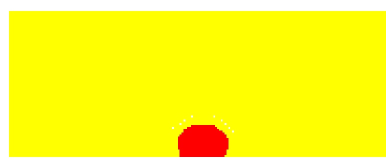
t=0.235 sec

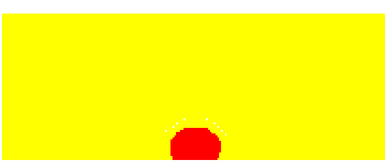
t=0.240 sec

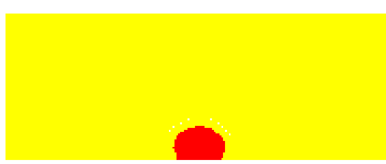
t=0.245 sec

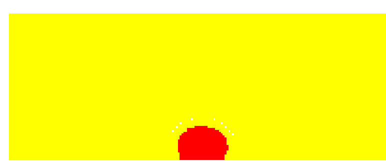
t=0.250 sec

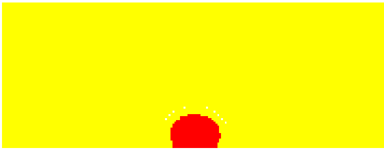
t=0.255 sec

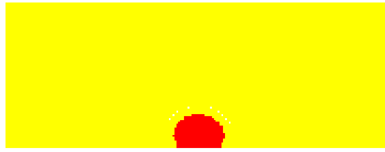
t=0.260 sec

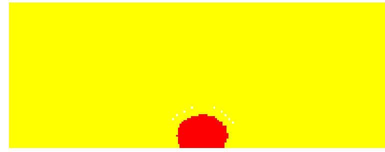
t=0.265 sec

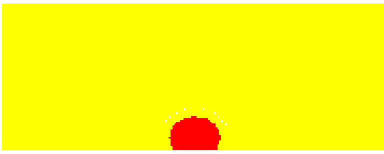
t=0.270 sec

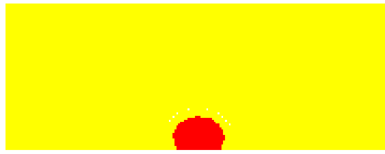
t=0.275 sec

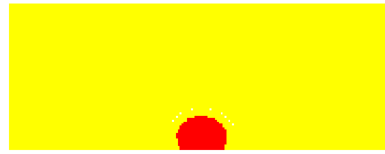
t=0.280 sec

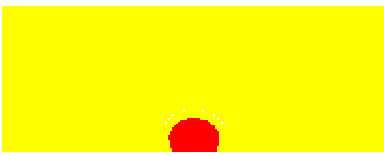
t=0.285 sec

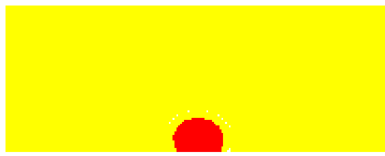
t=0.290 sec

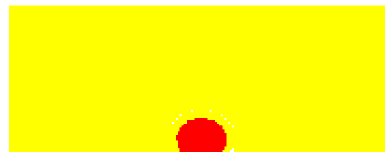
t=0.295 sec

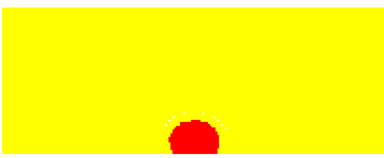
t=0.300

Figure 9: Equilibrium shapes of water drop over a horizontal plane with contact angle of 150^0.

The plots of contours of velocities are shown below in Figure 10:

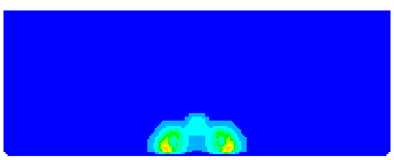
t=0.005 sec

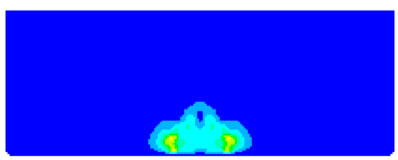
t=0.010 sec

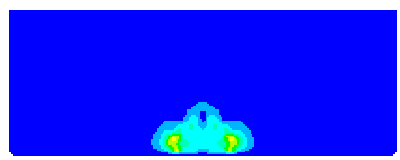
t=0.015 sec

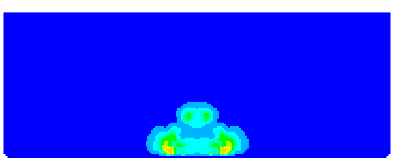
t=0.020 sec

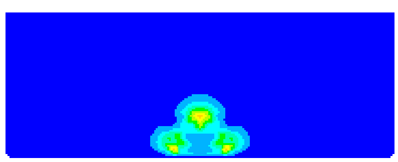
t=0.025 sec

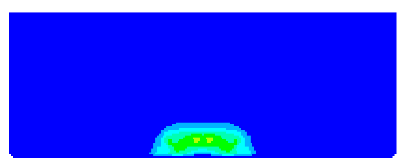
t=0.030 sec

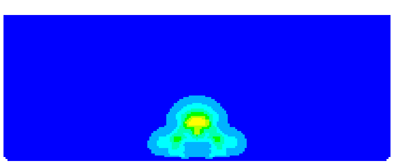

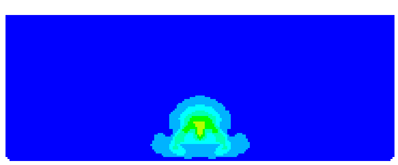

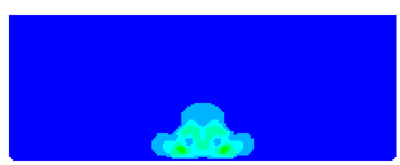

t=0.035 sec | t=0.040 sec | t=0.045 sec

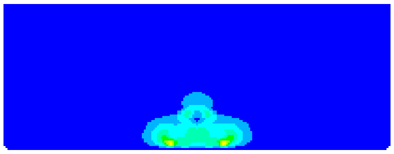 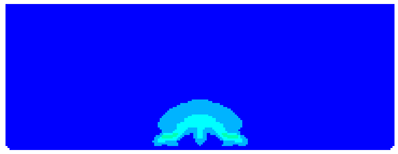 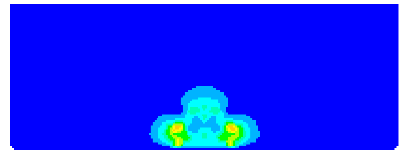

t=0.050 sec | t=0.055 sec | t=0.060 sec

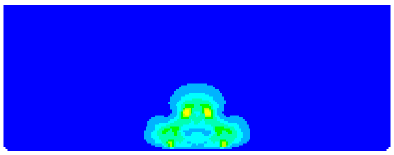 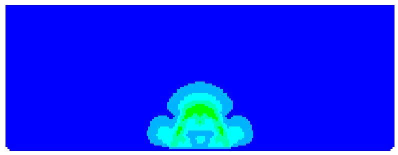 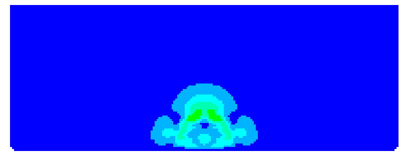

t=0.065 sec | t=0.070 sec | t=0.075 sec

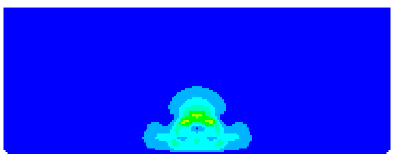 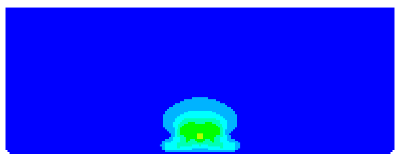 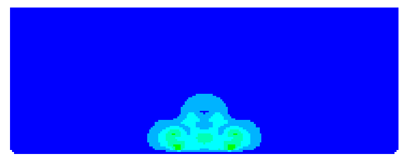

t=0.080 sec | t=0.085 sec | t=0.090 sec

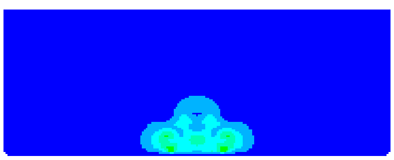 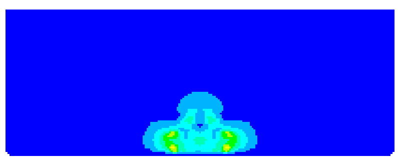 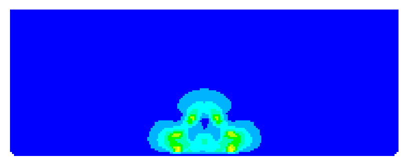

t=0.095 sec | t=0.100 sec | t=0.105 sec

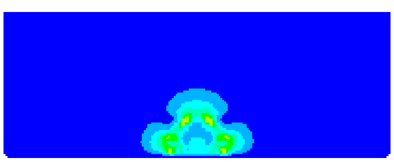 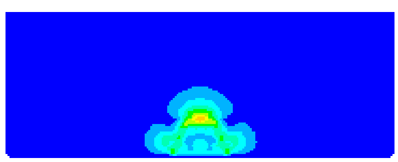 

t=0.110 sec | t=0.115 sec | t=0.120 sec

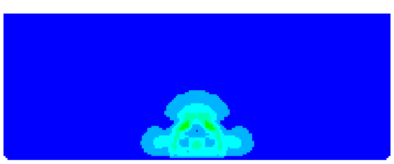 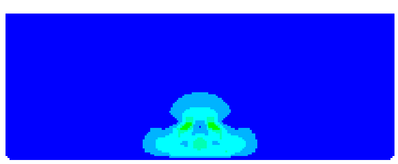 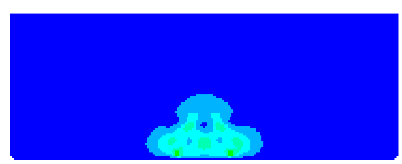

t=0.125 sec | t=0.130 sec | t=0.135 sec

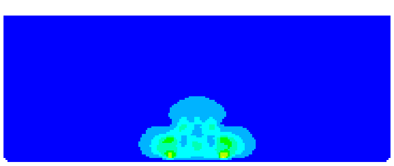 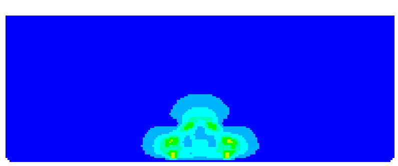 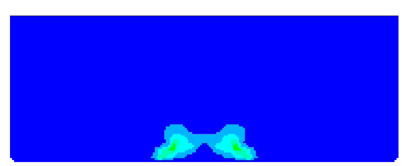

t=0.140 sec | t=0.145 sec | t=0.150 sec

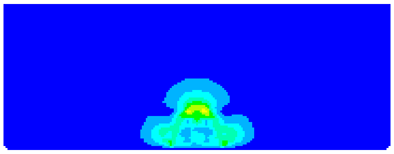
t=0.155 sec

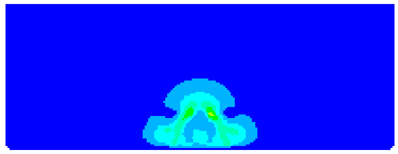
t=0.160 sec

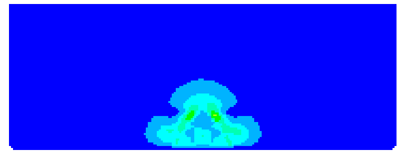
t=0.165 sec

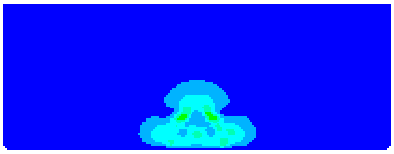
t=0.170 sec

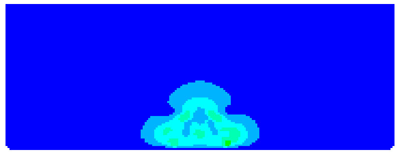
t=0.175 sec

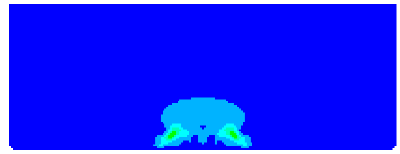
t=0.180 sec

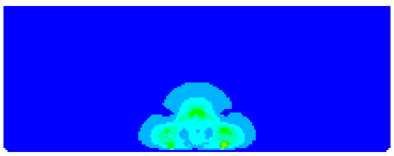
t=0.185 sec

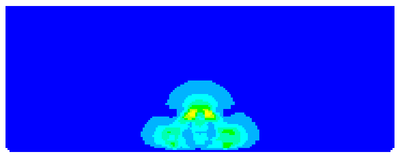
t=0.190 sec

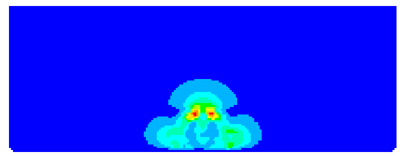
t=0.195 sec

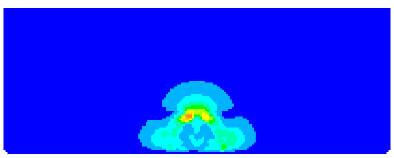
t=0.200 sec

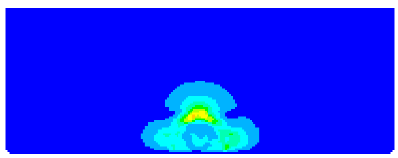
t=0.205 sec

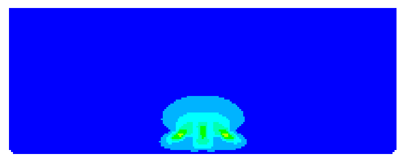
t=0.210 sec

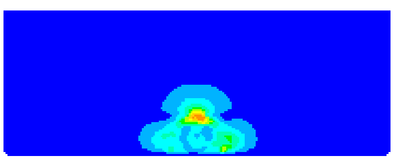
t=0.215 sec

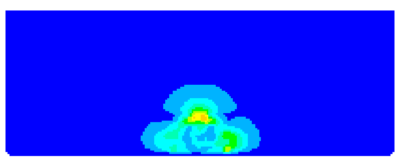
t=0.220 sec

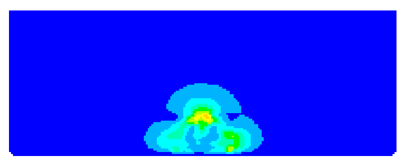
t=0.225 sec

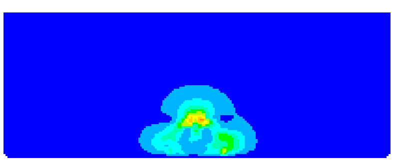
t=0.230 sec

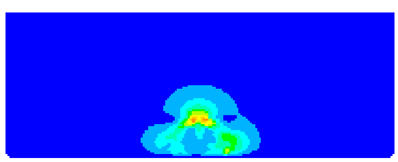
t=0.235 sec

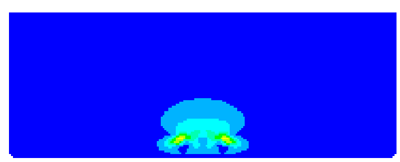
t=0.240 sec

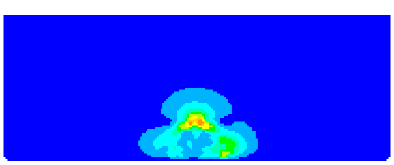
t=0.245 sec

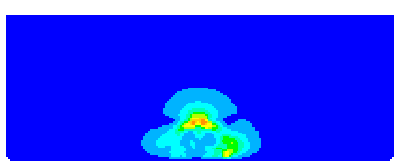
t=0.250 sec

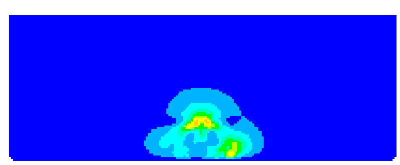
t=0.255 sec

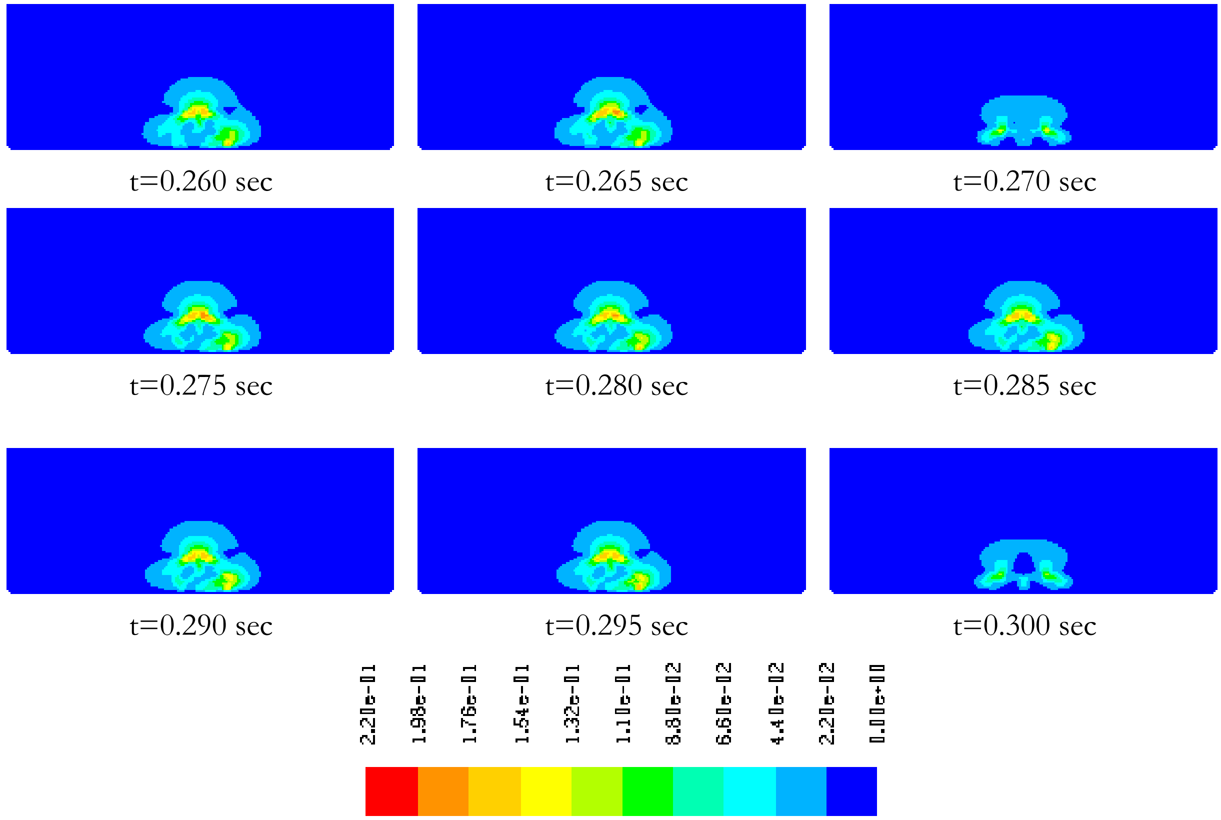

Figure 9: Velocity contours of drop over a horizontal plane with contact angle of 150^0.

In the second phase of analysis, till now six results on the critical angle at which the drop just tries to propel have been obtained as shown. Taking an example of determination of critical wettability gradient of a $1mm^3$ water drop the images below represent the movement with respect to time:

At wettability gradient of 16°/mm: (figure 11):

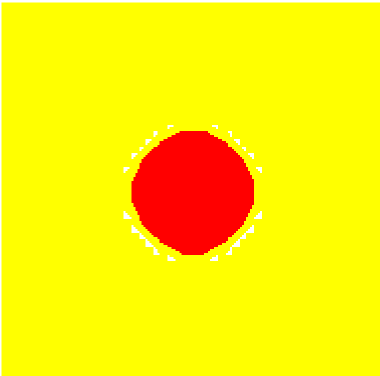

t = 0 sec

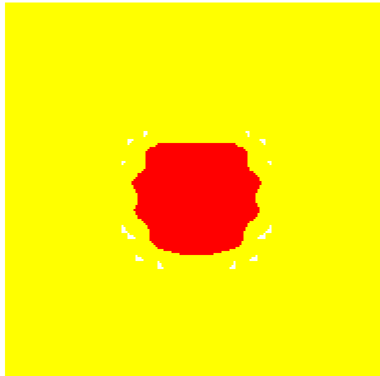

t = 0.02 sec

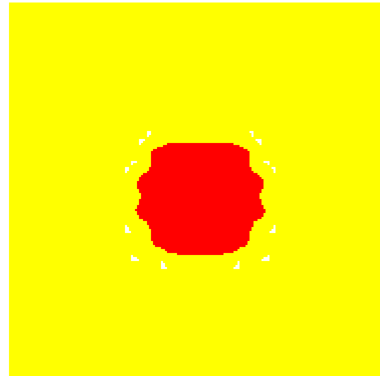

t = 0.04 sec

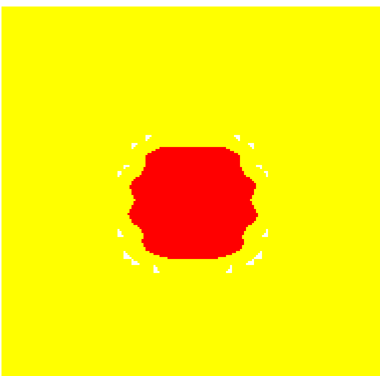

t = 0.06 sec

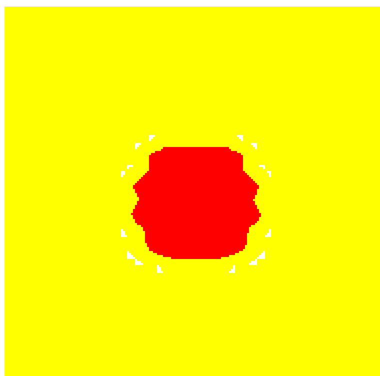

t = 0.08 sec

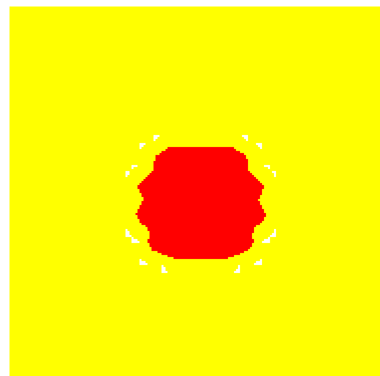

t = 0.10 sec

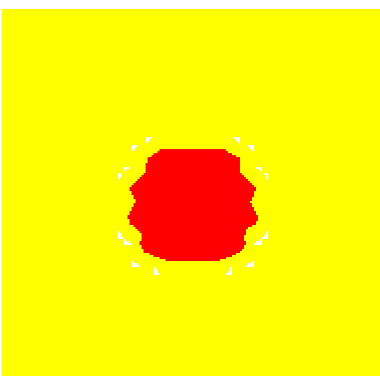

t = 0.12 sec

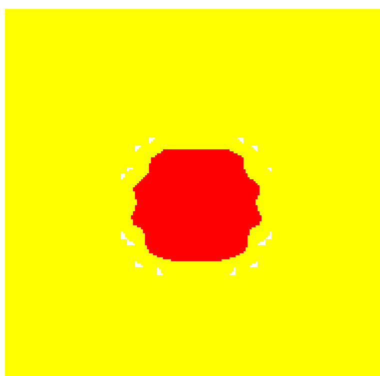

t = 0.14 sec

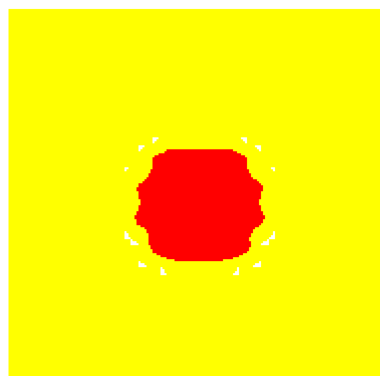

t = 0.16 sec

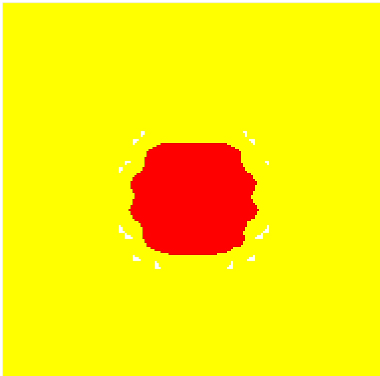

t = 0.18 sec

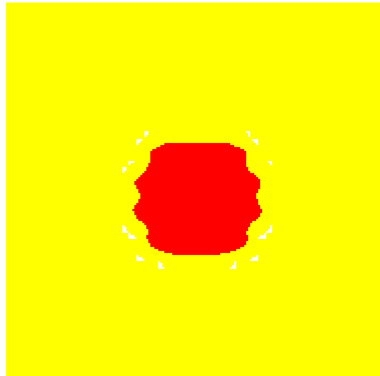

t = 0.20 sec

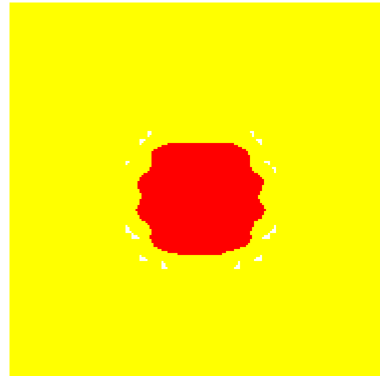

t = 0.22 sec

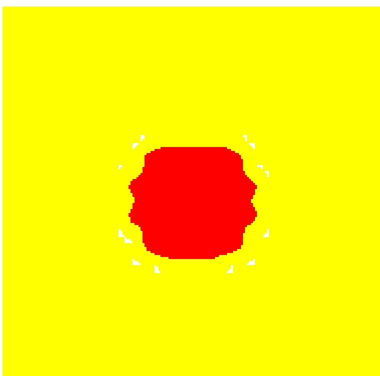

t = 0.24 sec

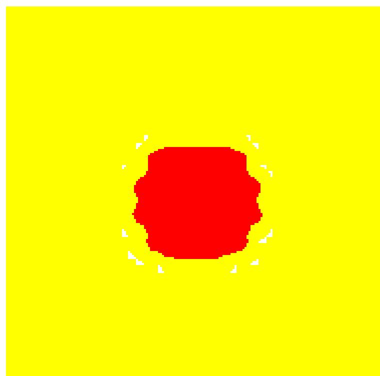

t = 0.26 sec

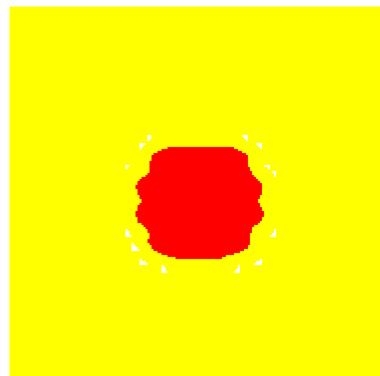

t = 0.28 sec

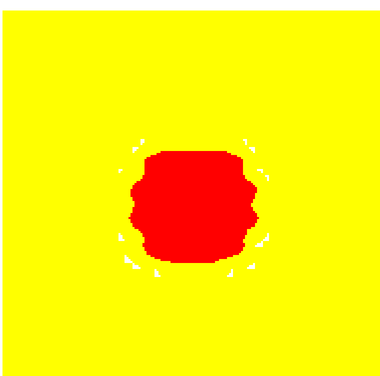

t = 0.30 sec

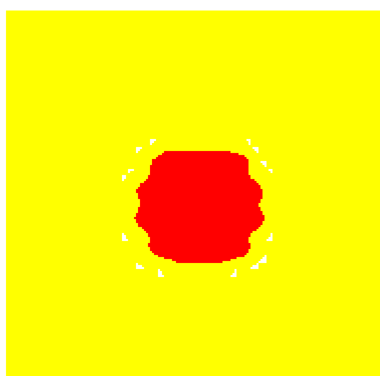

t = 0.32 sec

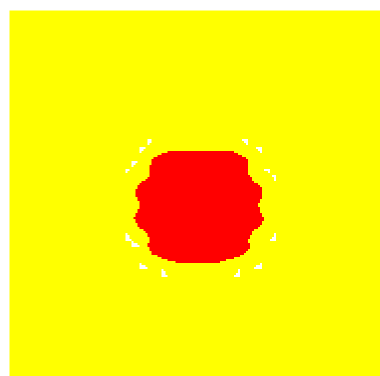

t = 0.34 sec

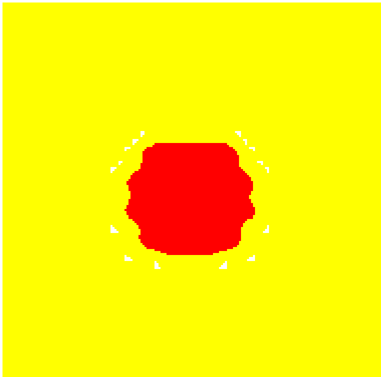

t = 0.36 sec

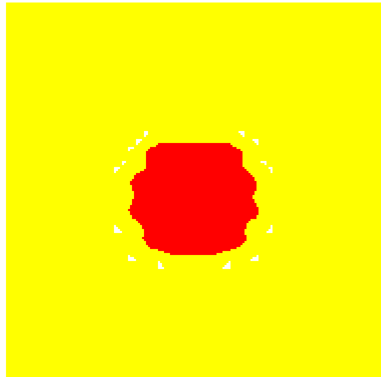

t = 0.38 sec

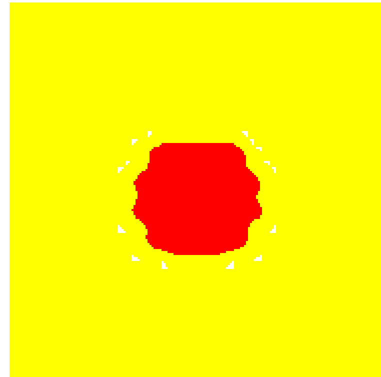

t = 0.40 sec

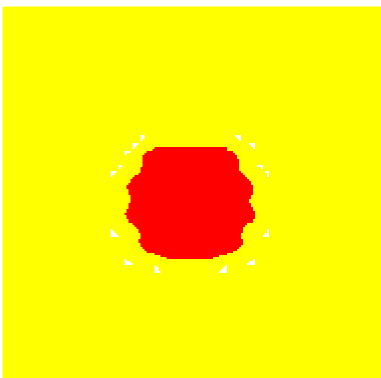

t = 0.42 sec

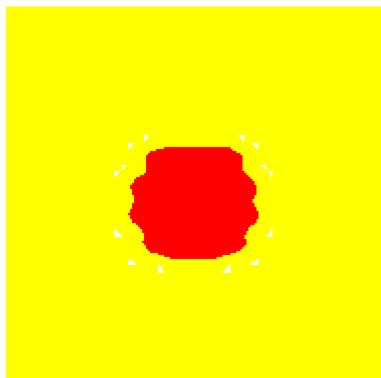

t = 0.44 sec

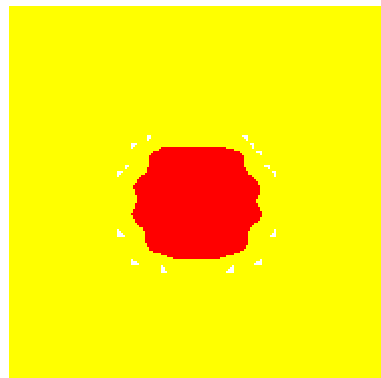

t = 0.46 sec

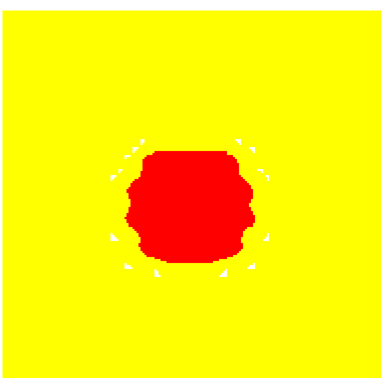

t = 0.48 sec

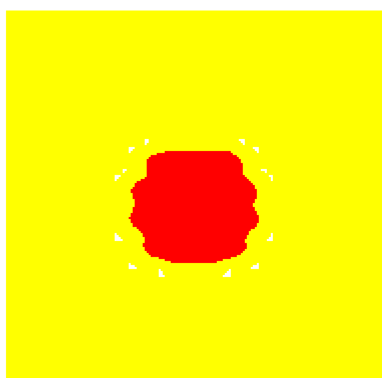

t = 0.50 sec

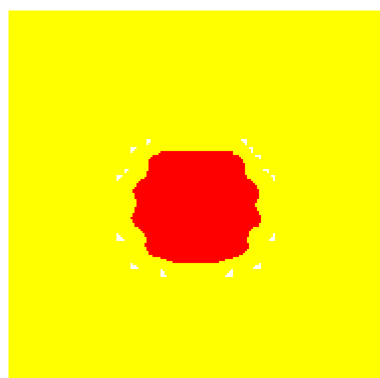

t = 0.52 sec

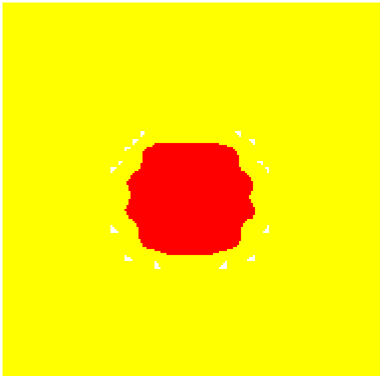

t = 0.54 sec

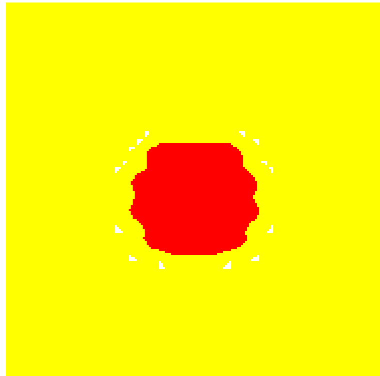

t = 0.56 sec

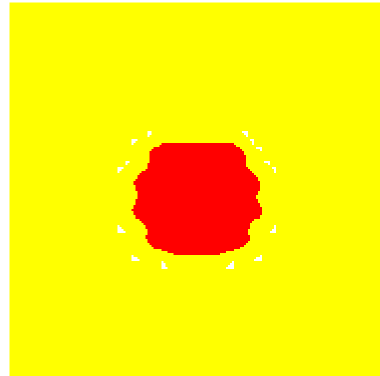

t = 0.58 sec

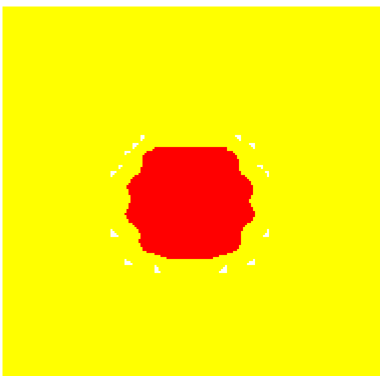

t = 0.60 sec

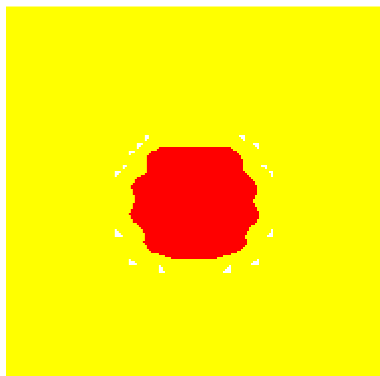

t = 0.62 sec

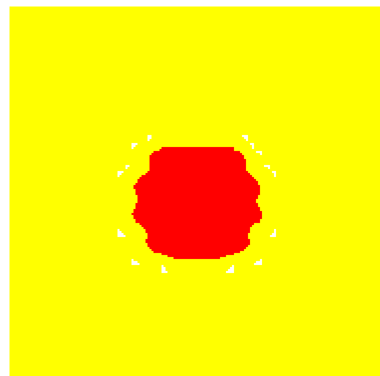

t = 0.64 sec

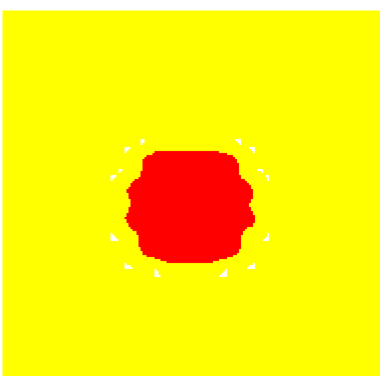

t = 0.66 sec

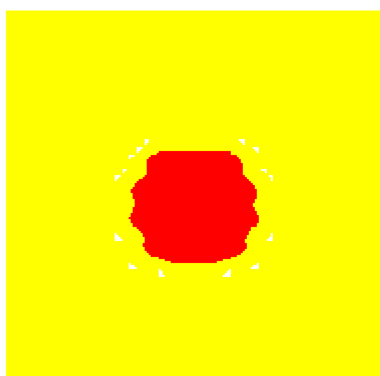

t = 0.68 sec

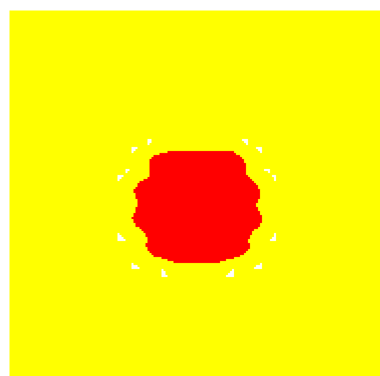

t = 0.70 sec

At wettability gradient of 17°/mm (Figure 12):

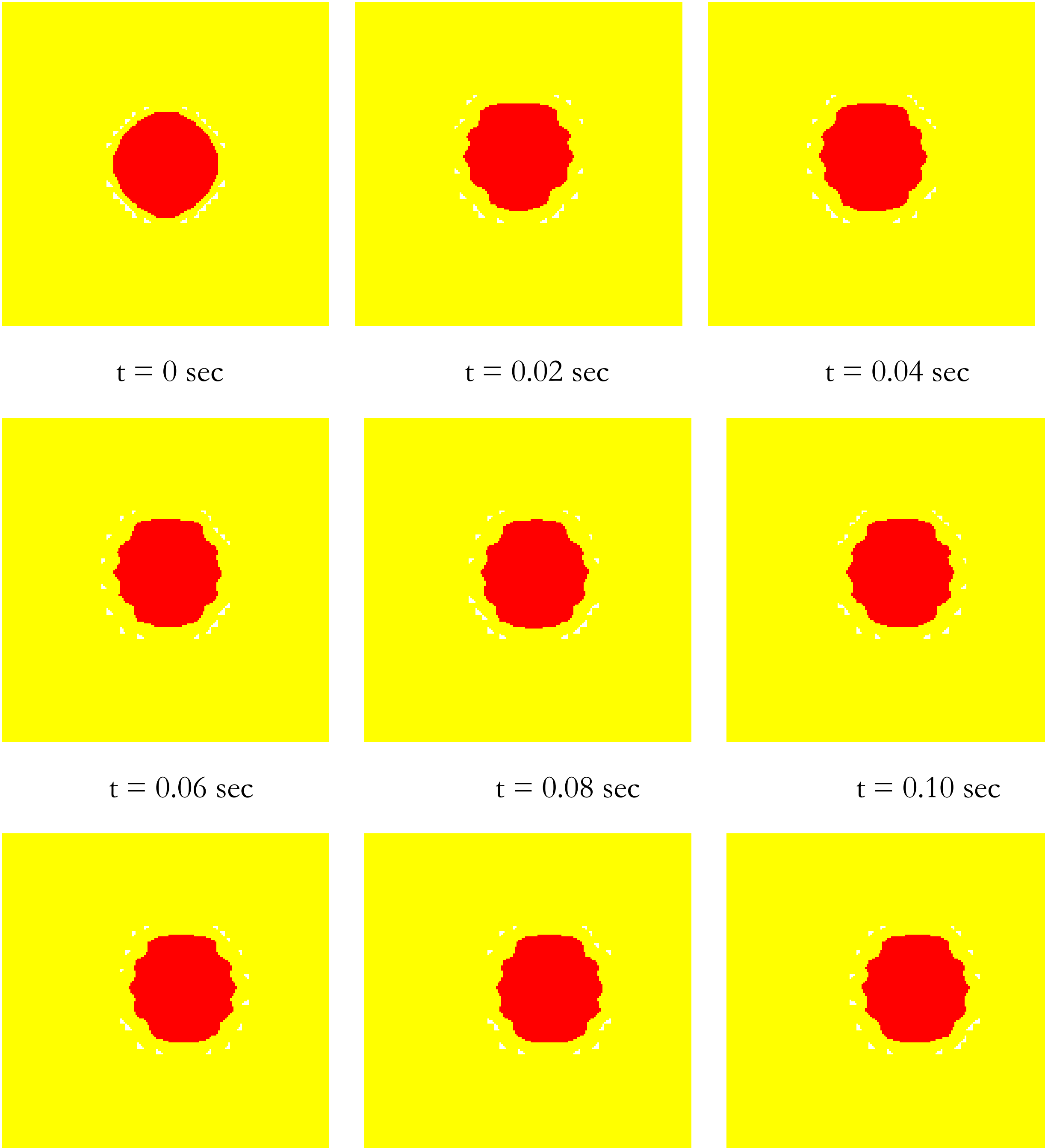

t = 0 sec

t = 0.02 sec

t = 0.04 sec

t = 0.06 sec

t = 0.08 sec

t = 0.10 sec

t = 0.12 sec

t = 0.14 sec

t = 0.16 sec

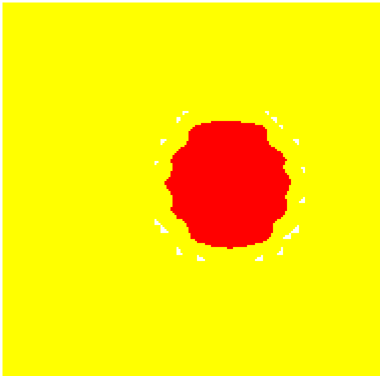

t = 0.18 sec

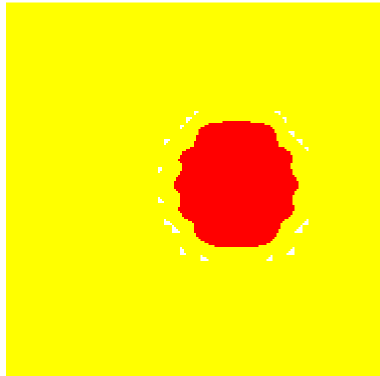

t = 0.20 sec

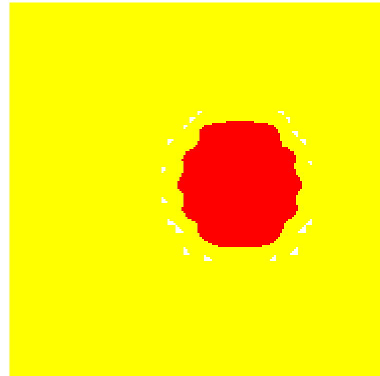

t = 0.22 sec

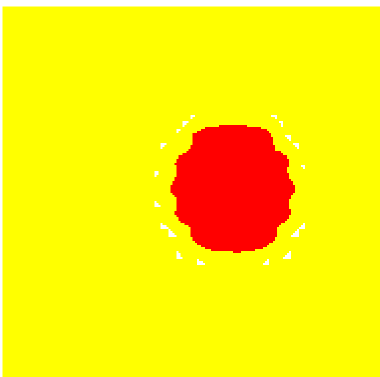

t = 0.24 sec

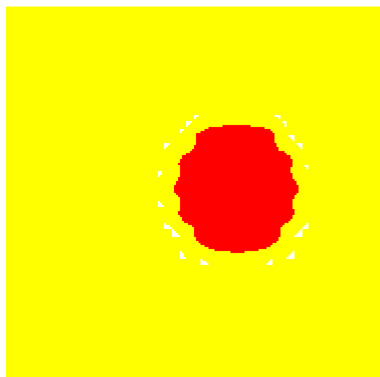

t = 0.26 sec

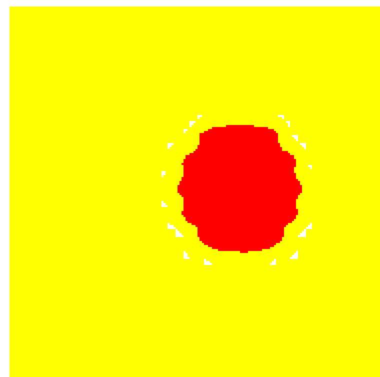

t = 0.28 sec

The results obtained are depicted in a tabular form below:

Volume(mm^3)	Critical Wettability gradient(°/mm)
1	17
6	9
8	6
17	5.5
20	8
50	10

Figure- 13

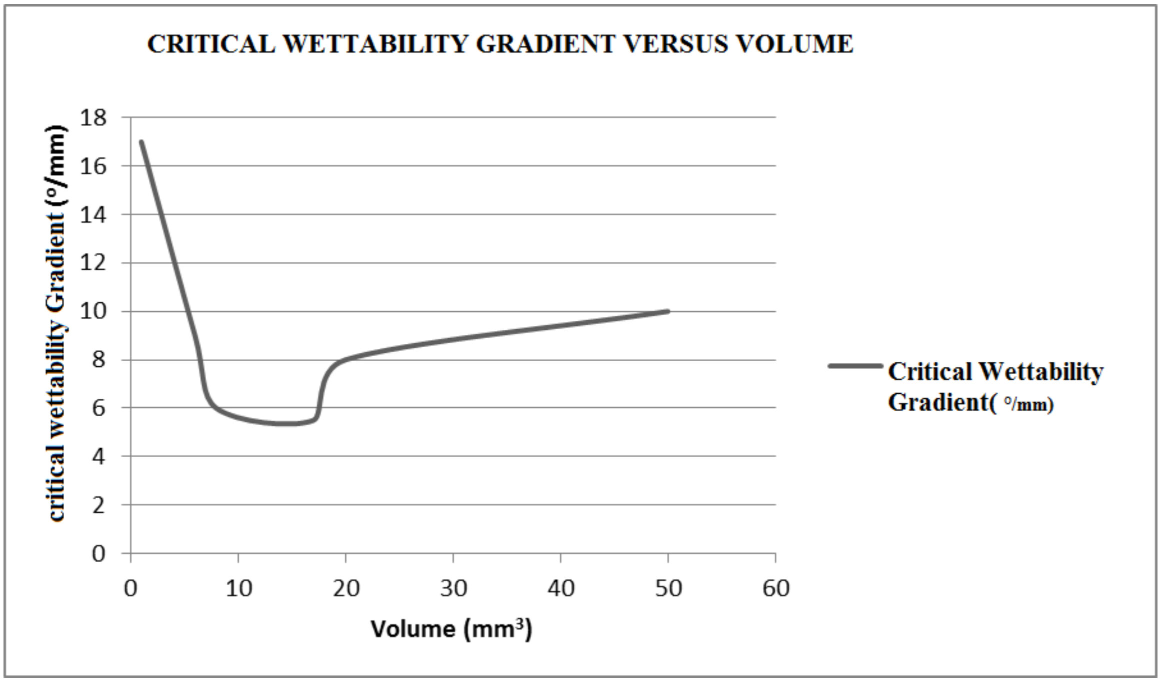

Figure-14

When plotted in graph, the curve represents a steep drop from left as shown, when volume increases from 1mm^3 and tries to obtain a minimum value a moderate volumes after which, it begins to rise gradually with increase in volume. Also it was observed that with increase in volume of the drop, the time at which it starts to propel, i.e., the time needed to stabilize itself from the initial hemi-spherical shape assumed to the final equilibrium shape increases with increase in volume of the drop.

Chapter 5

5. IMPORTANT CONCLUSIONS:

The equilibrium shape obtained by a variety of liquid-solid combinations are dependent upon a number of factors like surface tension, volume of the drop, surrounding atmosphere, material properties, external forces, contamination of the liquid and surface gradient. The equilibrium shape obtained serves as the base over which the prediction of the dynamics of the drop under the influence of an unsteady external force. Also, the stability of a drop over the surface can be predicted by this model. As could be inferred from the above results, the time required by the drop to attain equilibrium shape and the velocity pattern of the various particles can be plotted over the surface of the droplet. The flow pattern over the droplet may serve to explain the distribution of the particles which may help in analyzing the mixing behavior of various phases.

As could be inferred from the results above, as the volume increases (let's say beyond $10mm^3$), the wettability gradient has to be increased in order to account for the increase in inertial and viscous forces of the droplet, a consequence of increase in mass. But when we analyze the drop at lesser volumes it could be observed that inertial force has been overcome by the decrease in the contact surface area at the base which requires a very high driving force(a higher contact angle hysteresis), as indicated by the steep slope in the graph. In the second phase the gradual increase in time lag for the drop with increase in the volume is accounted by the fact that a higher volume droplet needs more time to attain stability, i.e., equilibrium state under external effects and upon attaining stabilization it takes up the established wettability gradient over the surface and propels itself. Also the movement of the droplet is a bit sluggish owing to its increased inertia and resistive viscous forces.

Chapter 6

6. FUTURE WORK:

The next phase of analysis part may be based on the application of various wettability gradient profiles (non-linear) over the liquid drop over a variety of surface and observation of the critical conditions to propel the drop and the velocity as a function of the applied wettability gradient. The effect of the change in volume of the droplet on the above factors would be analyzed and some mathematical model, if possible, would be proposed to account for the above factor. Also, simulations could be done taking inclined plane models and the critical conditions of volume and applied wettability gradient over the drop would be determined. Mobility curves representing inclination angle versus volume of the droplet such that it remains static under the opposing forces of gravity and wettability gradient would be plotted. The above results could be inferred from different material combinations and the pattern of variation could be analyzed to develop some theoretical model for correlation between them. The pattern of flow of the fluid particles over the various regions could be plotted as a function of time to study the flow patterns for various boundary conditions. Also, the flow of a drop over various profiles of solid surfaces (non-linear) could be simulated to analyze the nature of flow and the flow pattern over the surface of the droplet. The intermixing and separation of drops under the effect of external forces and geometry of the bounding surface could be studied which has a great potential as an applicant in the microelectronic circuits. Finally, the observed nature and behavior of the dynamics could be correlated for the requirements of any patent applications and to have a systematic advancement in this field of research.

Chapter 7

7. REFERENCES:

[1] Bartolo D, Boudaoud A, Narcy G. & Bonn D.,2007.Dynamics of non-Newtonian droplets, Phys. Rev. Lett. 99, 174502.

[2] Beltrame P, Hanggi P, Knobloch E Thiele U., 2001. Depinning of 2d and 3d droplets blocked by a hydrophobic defect.

[3] Brochard F., 1988. Motions of Droplets on Solid Surfaces Induced by Chemical or Thermal Gradients

[4] Chaudhury K. M,Whitesides M.G.,1992. How to make water Run uphill, Science, 256,1539-1541.

[5] Das A.K, Das P. K., 2010. Multimode Dynamics of a Liquid Drop over an Inclined Surface with a Wettability Gradient, Langmuir, 26, 9547–9555.

[6] Daniel S, Chaudhury M.K, Chen J.C., 2001. Fast drop movements resulting from the phase change on a gradient surface, Science, 291(5504),633-636.

[7] Dantel S, Chaudhury K.M., 2002. Rectified Motion of Liquid Drops on Gradient Surfaces Induced by Vibration, 18, 3404-3407.

[8] Denis Bartolo, Arezki Boudaoud, Gregoire Narcy, and Daniel Bonn.,2007. Dynamics of Non-Newtonian Droplets, 99, 174502-1, 174502-4.

[9] Ding, H. & Spelt, P. D. M., 2007. Inertial effects in droplet spreading: a comparison between disuse interface and level-set simulations, J. Fluid Mech., 576, 287-296

[10] Dussan V.E.B,Chow R.T.,1983. ability of drops or bubbles to stick to non-horizontal surfaces of solids,journal of fluid mechanics,137,1-29.

[11] Ford L. M, Nadim A., 1994. Thermo capillary migration of an attached drop on a solid surface, American Institute of Physics.

[12] Gallardo, B.S., Gupta, V.K., Eagerton,F.D., Jong, L.I., Craig, V.S,Shah, R.R. & Abbot, N.L.,1983.Electrochemical principles for active control of liquids on sub millimeter scales, Science ,283, 57-60.

[13] Gao.L, McCarthy J.T., 2006. Contact Angle Hysteresis Explained, Langmuir, 22, 6234-6237.

[14] Gingold R.A,Monaghan J.J.,1977, Smoothed particle hydrodynamics - Theory and application to non-spherical stars,Mon.Not.R.astr.Soc,181,375-389.

[15] Gau H, Herminghaus .S, Lenz.P,Lipowsky.R.,1999. Liquid Morphologies on Structured Surfaces, From Micro channels to Microchips, Science journal,283,46-49.

[16] Greenspan H.P, 1978. On the motion of a small viscous droplet that wets a surface, Journal of Fluid Mechanics,84,125-143.

[17] Holmes W.H, Williams R.J, Tilke P., 2000. Smooth particle hydrodynamics simulations of low Reynolds number flows through porous media, Int. J. Numer. Anal. Meth. Geomech, 1.02, 1-6.

[18] Hongwen R, 2010. Liquid crystal droplet array for non-contact electro-optic inspections, J. Phys. D: Appl. Phys, 43, 365103.

[19] Huang J.J, Shu C, Chew Y.T, 2008. Numerical investigation of transporting droplets by spatiotemporally controlling substrate wettability. J Colloid Interface Sci., 328, 124-133.

[20] Juncker, D., Schmid. H., Drechsler U., Wolf, H., Wolf, M., Michel, B., 2002. Autonomous Microfluidic Capillary System, Anal Chem,74,6139-6144.

[21] Kusumaatmaja, H, Yeomans, J. M., 2007. Modeling contact angle hysteresis on chemically patterned and superhydrophobic surfaces, Langmuir, 23, 6019-6032.

[22] Morris J.P, Fox P.J, Zhu Y.,1997. Modeling low Reynolds number incompressible °ows using SPH. Journal of Computational Physics, 136,214-226.

[23] Moumen N, Subramanian S.R, McLaughlin B.J, 2006. Experiments on the Motion of Drops on a Horizontal Solid Surface Due to a Wettability Gradient, Langmuir, 22, 2682-2690.

[24] Pismen L.M,Thiele U.,2006, Asymptotic theory for a moving droplet driven by a wettability gradient Phys. Fluids 18, 042104-14.

[25] Shikhmurzaev D.Y.,1997. Moving contact lines in liquid/liquid/solid systems,J. of fluid mechanics,334,211-249.

[26] Subramanian S.R., Moumen N., McLaughlin B.J., 2005. Motion of a Drop on a Solid Surface Due to a Wettability Gradient, Langmuir, 21, 11844-11849.

[27] Wu X, Thien N.P, Fan X.J, and Ng T.N.,2003. A molecular dynamics study of drop spreading on a solid surface, Phys. Of fluids,15,10.1063-10.1069.